PROX KINETICS OVER Pt-Sn/AC UNDER FULLY REALISTIC REACTION CONDITIONS

by

Belkız Merve Eropak

B.S. in Ch.E., Boğaziçi University, 2009

Submitted to the Institute for Graduate Studies in
Science and Engineering in partial fulfillment of
the requirements for the degree of
Master of Science

Graduate Program in Chemical Engineering

Boğaziçi University

2011

to my family

ACKNOWLEGMENTS

First of all, I would like to express my truthful gratitude to my thesis supervisor Prof. Ahmet Erhan Aksoylu, who devoted his valuable time to guiding me, helping me and motivating me all the time. It was a great opportunity for me to work with him during my thesis, where I learned from him great expertise and experiences in catalysis and reaction engineering. I am very grateful to Prof. Aksoylu for his real support in every condition. I also thank to Assoc. Prof. Ahmet K. Avcı and Assoc. Prof. Hasan Bedir, who has read and commented on my thesis.

Special thanks to Feyza Gökaliler and Burcu Selen Çağlayan, who devoted their valuable time to guide and help me all the time. I also wish to express my gratitude to other members of 411/A group, Tuğba Davran Candan, Ali Uzun, Vasfiye Çimenoğlu, Nilay Aktürk and Murat Erol for their suggestions and friendships.

Heartfelt thanks to my comrades, İhsan Ömür Akdağ, Melek Selcen Başar, Aslıgül Doğan, Gülsüm Ersoy, Mehmet Ünal Güneş, Mehmet İrfan Hösükoğlu, Duygu Kocaman, Aybüke Leba, Çağlar Meriçer, Bahar Nalbantoğlu, Şefik Kerem Ovalı, İpek Paksoy, Caner Ülgüel, Simay Yalaz, Burcu Yoğurtçu, Okan Yüzüak for giving me their everlasting friendship and joyful help all the time.

Cordial thanks for Bilgi Dedeoğlu and Nurettin Bektaş for their technical assistance and significant efforts during my thesis and also Yakup Bal for his friendly attitude.

Finally, I would like to thank my family for their unrequited support and trust in me throughout my thesis like my whole life. This work is dedicated to them, without whom it would have never been possible.

The graduate scholarship provided by TÜBİTAK for my M.S. studies deserves thankful recognition. Financial support provided by TÜBİTAK through project 105M282, by Boğaziçi University through project BAP 09M104, and by State Planning Organization of Turkey through project DPT 07K120630 are gratefully acknowledged.

ABSTRACT

PROX KINETICS OVER Pt-Sn/AC UNDER FULLY REALISTIC REACTION CONDITIONS

This experimental study comprises a kinetic study of preferential CO oxidation (PROX) in the presence of H_2, CO_2, H_2O, and CH_4 over HNO_3-oxidized activated carbon supported 1wt.%Pt 0.25wt.%Sn/AC catalyst prepared by the sequential impregnation method. In this context, kinetic experiments were conducted at 383 K and atmospheric pressure, and different sets of CO and O_2 concentrations, each at different space times and catalyst loadings, were used. Molar reactant concentrations in the feed were varied between 1-2.5 per cent CO and 1-1.5 per cent O_2. The effects of CO flow rate, O_2 flow rate, and λ (O:CO) on CO conversion were also investigated for various experiments ranging λ from 1 to 3. Experimental rate data were used to estimate kinetic parameters of the power-law kinetic model by using the method of initial rates. The investigation of power-law kinetics gave reaction orders of 0.29 and 0.17 with respect to carbon monoxide and oxygen, respectively, at 383 K. The variance of experimental error was found to be 0.1019 $(\mu mol.mg^{-1}.min^{-1})^2$ for this rate expression, which indicates that experimentally measured and model predicted rates was not perfectly fitted most probably due to the presence of a secondary mechanism through water activation involving surface OH^- group, which has been confirmed by DRIFT studies in the production of surface oxygen; thus although H_2, CH_4, CO_2, and H_2O amounts in the feed is fixed, the surface mechanism may still be affected especially by CO/H_2O and O_2/H_2O feed ratios. The activation energy was predicted as 42.3 kJ mol^{-1} and the frequency factor was calculated as $1.44\times10^5\ \mu mol\ mg^{-1}\min^{-1}\ kPa^{-0.46}$. As the calculated orders with respect to CO and O_2 in the current study are widely different from the previous one on the same catalyst with a feed having only CO and O_2, which were 0.96 and (-0.31), respectively; the crucial importance of having a kinetic expression, which is valid for real feed, in the PROX reactor design has been confirmed.

ÖZET

GERÇEK REAKSİYON KOŞULLARI ALTINDA AKTİF KARBON DESTEKLİ Pt-Sn KATALİZÖRÜ ÜZERİNDE SEÇİMSEL KARBONMONOKSİT OKSİDASYONU KİNETİĞİ

Bu deneysel araştırma, ardışık emdirilme yöntemiyle hazırlanmış ve nitrik asit ile yükseltgenmiş aktif karbon destekli ağırlıkça 1%Pt-0.25%Sn içeren katalizör üzerinde hidrojen, karbondioksit, su ve metan varlığında yapılan seçimsel karbonmonoksit oksidasyonu (PROX) kinetik çalışmasını içermektedir. Kinetik deneyler 383 K sıcaklıkta ve atmosferik basınç altında yapılmış, kinetik ölçümlerde farklı karbon monoksit ve oksijen yüzdeleri ile her bir konsantrasyon için farklı reaktörde kalma süreleri ve katalizör miktarları kullanılmıştır. Beslemedeki reaktant konsantrasyonları karbonmonoksit için yüzde 1 ile 2.5 arasında, oksijen için yüzde 1 ile 1.5 arasında değiştirilmiştir. Ayrıca karbonmonoksit akış hızının, oksijen akış hızının ve deneylerde 1 ve 3 arasında değişen oksijen karbonmonoksit oranının, karbonmonoksit dönüşümüne etkisi araştırılmıştır. Deneysel hız verileri kullanılarak üssel hız denkleminde yer alan kinetik parametreler başlangıç hızları yöntemi ile hesaplanmıştır. üssel hız denklemi araştırması, 383 K sıcaklığında karbonmonoksit ve oksijenin reaksiyon mertebelerini sırasıyla 0.29 ve 0.17 olarak belirlemiştir. Bu hız ifadesi için deneysel hata varyansı 0.1019 $(\mu mol.mg^{-1}.min^{-1})^2$ olarak bulunmuş olup büyük olasılıkla DRIFT çalışmalarıyla da onaylanan yüzey oksijen üretiminde, yüzey OH^- grubu barındıran su aktivasyonundan dolayısıyla oluşan ikinci bir mekanizmanın varlığından dolayı, deneysel olarak ölçülen ve kinetik parametrelerle yeniden hesaplanan hızlar mükemmel bir uyum göstermedi, bu nedenle beslemedeki H_2, CH_4, CO_2, and H_2O miktarları sabit tutulmasına rağmen, özellikle CO/H_2O ve O_2/H_2O oranlarından etkilenebilir. Aktivasyon enerjisi 42.3 kJ. mol^{-1} ve frekans faktörü $1.44\times10^5\ \mu mol\ mg^{-1}\ \min^{-1}\ kPa^{-0.46}$ olarak öngörülmüştür. Bu çalışmada elde edilen kinetik denklemdeki CO ve O_2 üstellerinin daha önce sadece CO ve O_2 içeren besleme koşulları altında elde edilen üstellerden, sırasıyla 0.96 ve (-0.31) oldukça farklı olması; PROX reaktörünün tasarımı için elde gerçek besleme koşulları için geçerli bir kinetik ifadenin bulunmasının hayati önemini teyid etmektedir.

TABLE OF CONTENTS

LIST OF FIGURES

LIST OF TABLES

LIST OF ABBREVIATIONS

AC	Activated Carbon
AFC	Alkaline Fuel Cell
BOS	Birleşik Oksijen Sanayi
CTR I	Packed Concentric Column
DOE	U.S. Department of Energy
DRIFTS	Diffuse reflectance IR Fourier Transform Spectroscopy
FP	Fuel Processor
GC	Gas Chromatograph
HPLC	High Performance Liquid Chromatography
HTS	High Temperature Shift Reaction
LTS	Low Temperature Shift Reaction
MCFC	Molten Carbonate Fuel Cell
PAFC	Phosphoric Acid Fuel Cell
PEM	Polymer Electrolyte Membrane
PEMFC	Proton Exchange Membrane Fuel Cell
PROX	Preferential Oxidation
RWGS	Reverse Water Gas Shift Reaction
SOFC	Solid Oxide Fuel Cell
T	Temperature
TCD	Thermal Conductivity Detector
TPD	Temperature Programmed Desorption
TOS	Time-on stream
WGS	Water-Gas Shift Reaction
XPS	X-ray Photon Spectroscopy

1. INTRODUCTION

Fuel cell (FC) has been drawing strong attention as an alternative power source generating electricity in a direct way for its potential higher efficiency and practically zero emissions (Caputo *et al.*, 2006). Hydrogen is an ideal fuel for fuel cells due to its high reactivity and zero emission characteristics. Since safe and efficient storage technology for hydrogen is currently not available, it can be generated from natural gas, gasoline or alcohols using an (on site) fuel processor (FP) (Mariño *et al.*, 2004). On site hydrogen production via FP seems to be the most promising and suitable alternative to compensate the disadvantage of hydrogen storage (Moreño *et al.*, 2008). Thus, the use of combined FP-FC systems in distributed energy production is expected to be well proliferated in the near future.

Proton exchange membrane fuel cells are one of the most viable fuel cell technologies for small scale stationary applications like energy and/or combined heat and energy generation in houses, apartments, etc., since it has high density, small volume and it works at lower temperature ranges. The preferential oxidation of CO in a H_2-rich atmosphere has gained importance in the combined "FP-PEMFC" technologies considering the fact that PEM needs ppm level CO concentrations for stable operation (Suh *et al.*, 2005). Decrease in CO level is required to avoid the poisoning of the Pt anode of a conventional low temperature PEM fuel cell. In general maximum, allowable CO level in the hydrogen feed for stable operation of PEM is between 10-50 ppm depending on catalysts used in PEMFC (Kolb *et al.*, 2007).

In hydrogen production from hydrocarbons by using FPs, significant amount of CO production is unavoidable as the hydrogen is produced and enriched by the series of catalytic reforming and water-gas shift units of the fuel processor. Complete removal of CO from the H_2 stream produced is a necessity (Baltacıoğlu *et al.*, 2007). After the reformer, CO is partially converted to CO_2 in the water gas shift reactor (WGS), but the conversion level is limited by thermodynamics, which means further purification treatments are required (Mariño *et al.*, 2004). Several available methods can be applied for CO removal such as methanation, Pd-based membranes and selective CO oxidation.

Among them, selective CO oxidation (Preferential CO oxidation, PROX) seems to be the most effective owing to its relatively simple implementation, lower operating costs and minimal hydrogen loss (Avcı *et al.*, 2001). The gas exits from the water gas shift reactor, which will be fed to the PROX reactor includes 50-75 vol% H_2, 10-20 vol% CO_2, 5-10 vol% H_2O and 0.5-1 vol% CO. The CO level must be reduced down to a level 10-50 ppm by the PROX reactor in order to avoid the deactivation of the electrodes of the PEM fuel cells. The selectivity in PROX reactor is also a major objective since hydrogen oxidation may also occur besides CO oxidation (Caputo *et al.*, 2007).

In order to achieve the required selectivity, catalysts with high activity of carbon monoxide removal with suppressed hydrogen oxidation selectivity should be developed and used. In general, supported noble metal catalysts are used in these systems owing to the fact that they selectively enhance the CO oxidation (Baltacıoğlu *et al*., 2007). In the design of the fuel processor's reforming, WGS and PROX reactors, in the dynamic modelling of their serial operation, and in the design of the central control module to be used during combined FP-PEMFC operation; reliable, catalyst-specific kinetic expression for each of these reactors under realistic operation conditions are needed**.**

Inactivity of conventional CO oxidation catalysts at low temperatures has given rise in the interests of the researchers for developing new catalysts. An efficient low temperature CO oxidation catalyst should accommodate CO chemisorption and the simultaneous dissociative adsorption of O_2. This has suggested the use of composite materials with different components each having activity for one of these functions (Trimm and Önsan, 2001). A series of catalysts and supports have been investigated in order to determine suitable catalysts for the selective oxidation of carbon monoxide in hydrogen rich streams. Catalysts used for low-temperature CO oxidation in hydrogen-rich streams generally consist of a noble metal, i.e. platinum, palladium, ruthenium, etc., a reducible metal oxide, i.e. transition metal oxides, etc., and the support material. Our recent experimental studies revealed that Pt-Sn system supported on HNO_3-oxidized activated carbon (AC3) has superior and stable activity at 110^0C-135^0C temperature range under the flow of streams having composition of WGS outlet (i.e. fully realistic stream).

The aim of this work was to study the kinetics of PROX over AC3 supported 1wt%Pt-0.25wt%Sn under fully realistic conditions and to obtain a reliable, power-law type rate expression to be used in PROX reactor modelling and design calculations. Kinetic studies have been conducted in the initial rates region at a temperature of 383 K. A power function rate expression has been established with experimentally determined reaction orders with respect to CO and O_2. Effect of CO and O_2 concentration in the feed, and also O:CO ratio on the activity has also been investigated.

Chapter 2 contains literature survey including information about fuel cells and H_2 production followed by detailed information about preferential CO oxidation and also active and selective catalysts for this reaction. The experimental procedures used in the present study are presented in Chapter 3. The results obtained in the experiments and related discussions can be found in Chapter 4. Finally, Chapter 5 consists of the conclusions drawn from the present study and recommendations for future work.

2. LITERATURE SURVEY

2.1. Fuel Cells

A fuel cell is an electrochemical device that combines hydrogen passes over one electrode and oxygen passes over the other one, to produce electricity with water and heat as its by-product. The operation of a fuel cell is continuous as long as the fuel and other necessary reactants are supplied. Its operation is similar to a battery, but it does not have need of recharging or it does not run down. Fuel cells have many applications such as fuel cell powered-cars, buses, planes and vending machines. There are stationary applications including telecommunication sector, landfills and wastewater treatment plants.

Fuel cells can take the place of batteries via providing 1kW to 5kW power for telecom sites without noise and emissions. Electronic systems can benefit from on-site or direct DC power supply that is provided by such systems (Kevin, 2011).

There are different types of fuel cells that contribute different applications. One of them is Proton Exchange Membrane fuel cell (PEM), which operates at low temperatures (350K) and are suitable for applications that need quick start-up such as automobiles. U.S. Department of Energy (DOE) indicates that these cells as the potential for replacement of rechargeable batteries. Some other kinds are Phosphoric Acid fuel cell (PAFC), Molten Carbonate fuel cell (MCFC), Alkaline fuel cell (AFC**),** and Solid Oxide fuel cell (SOFC) (Kevin, 2011).

PAFC operates at about 505K and it can use impure hydrogen as fuel. PAFCs can tolerate a CO concentration of about 1.5 percent. MCFCs use molten carbonate salt mixture electrolyte and operates relatively high temperatures (920K). Due to the high temperature requirement, they are not suitable for home use and mobile applications**.** AFCs use potassium hydroxide as the electrolyte and operate at 345 K. However, they require pure hydrogen and oxygen because of the sensitivity to carbon contamination. SOFCs use solid metal oxides as the electrolyte, and operate at very high temperatures - around 1800°F and are suitable for stationary applications (Kevin, 2011).

In PEM-FC technology, CO removal step is required for its hydrogen feed in order to avoid rapid deactivation of the platinum-electro catalyst in the PEM-FC, since anode catalyst of the fuel cell is sensitive to even traces of CO.

2.2. Hydrogen Production

Recently, hydrogen use is emphasized as an important clean and environmentally benign energy carrier and it is tried to take the place of traditional hydrocarbon fuels, regarding the advantages of hydrogen such as reducing the greenhouse gas emissions, high energy content and economic extent among hydrocarbon fuels (Cormos, 2011). Hydrogen is a very reactive element that is available in the universe abundantly, however it is in the form of water (H_2O), or fossil fuels. Hence it is a secondary form of energy, that is produced using other sources such as hydrocarbons. Due to the fact that fuel cell operation technology depends on the availability of hydrogen, hydrogen production technologies gained importance for electric generation through the use of new technologies like combined fuel processor- fuel cell systems (Koroneos *et al.*, 2004).

Hydrogen production can be performed by reforming a hydrocarbon fuel into a hydrogen rich gas mixture. Fuel processing procedure consists of reforming, water-gas shift and CO elimination stages (Ersöz *et al.*, 2006). There are several methods for hydrocarbon reforming, namely steam reforming, partial oxidation reforming, and autothermal reforming. The conversion of hydrocarbon fuels to hydrogen can be carried out by three main reactions in series: (i) reforming reaction; (ii) water gas shift reaction; and (iii) a preferential oxidation reaction, all of which are combined in catalytic devices called fuel processors (Sopeña *et al.*, 2007). All three catalytic stages are required in order to reduce CO level to fuel-cell requirements.

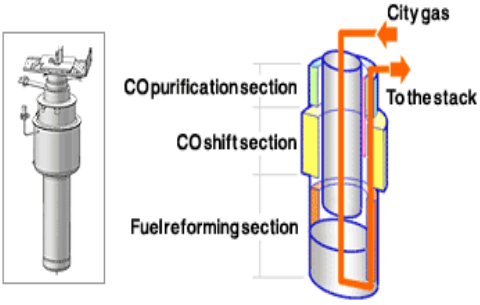

Figure 2.1. Fuel Processor.

2.3. Hydrogen Production Reactions

Hydrogen is generally derived form hydrocarbons by means of steam reforming, partial oxidation or autothermal reforming. Catalytic steam reforming is an old and well-known method for hydrogen production. The reaction (Eqn 2.1) is considerably endothermic and carried out at a temperature range of 700-850 ^{0}C. Partial oxidation reaction (Eqn 2.2) has an advantage, i.e. there is no need for external heat sources. Carbon deposition and slow kinetics are the main drawbacks of this reaction (Soykal, 2006).

$$C_nH_m + H_2O \longleftrightarrow n\,CO + (n + m/2)\,H_2 \qquad \Delta H^0_{298} > 0 \qquad (2.1)$$

$$C_nH_m + n/2\,O_2 \longleftrightarrow n\,CO + m/2\,H_2 \qquad \Delta H^0_{298} < 0 \qquad (2.2)$$

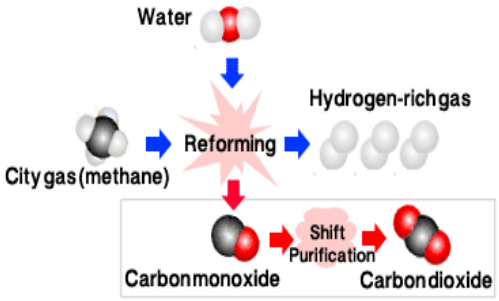

Figure 2.2. Hydrogen Production Mechanism.

In order to control the heat requirement and soot formation, steam reforming and oxidation reactions are coupled, and named as autothermal reforming. Therefore, energy produced by the second reaction, can be used in the first one (Soykal, 2006).

The second step of the catalytic CO-free hydrogen production from hydrocarbons is the water-gas shift reaction (Eqn 2.3). The CO produced in the reforming reaction, is reacted with steam over a catalyst to form extra hydrogen and carbondioxide.

$$CO + H_2O \longleftrightarrow H_2 + CO_2 \qquad \Delta H^0_{298} = 41.2\ kJ/mol \qquad (2.3)$$

As WGS is an equilibrium reaction, shift process is conventionally separated into two parts as high temperature shift reaction (HTS) taking place at 350 ^{0}C and low

temperature shift reaction (LTS) at 190-210 ^{0}C to benefit from high activity at high temperature and high conversion levels reached at low temperature.

Preferential oxidation step is needed to minimize the CO content. In this section, CO oxidation (Eqn 2.4) is tried to be maximized, whereas hydrogen oxidation (Eqn 2.5) is tried to be minimized.

$$CO + 1/2\ O_2 \longrightarrow CO_2 \qquad \Delta H^0_{298} = -282.984\ kJ/\ mol \qquad (2.4)$$

$$H_2 + 1/2\ O_2 \longrightarrow H_2O \qquad \Delta H^0_{298} = -241.818\ kJ/\ mol \qquad (2.5)$$

(Park *et al.*, 2009)

2.4. Preferential CO Oxidation (PROX)

Complete removal of CO present in the exit of water-gas shift product rich in H_2 is an essential requirement when the produced hydrogen is to be used as fuel to PEM fuel cells. The CO level in the downstream of the reformer is reduced by the shift reactions, but further CO removal is a must in order to decrease CO content from ca. 1-1.5% to below 10 ppm with minimal H_2 consumption (Suh *et al.*, 2005). The composition of the exit stream gases of water-gas shift reactors is 60-65% H_2, 10-15% H_2O, 1-2% O_2, rest CO_2 and inert (Schubert *et al.*, 2001). Hydrogen oxidation reaction is more exothermic than CO oxidation; thus, it is favored higher temperatures than CO oxidation and the activity of the selective CO oxidation catalysts should be high at low temperatures (Ratnasamy *et al.*, 2004).

2.5. PROX Catalysts

2.5.1. Monometallic PROX Catalysts

The most active CO oxidation catalysts that researchers have been agreed on are the noble metal catalysts such as Pt, Ir, and Pd. In the paper written by Mariño *et al.*, it was shown that Pt and Ir catalysts were more active and selective catalysts in a wide temperature range compared to Pd catalysts. The main drawback of the noble metals for being used in PROX is that they adsorb all the reactants involving H_2. As the temperature

increase enhances the hydrogen oxidation, Pt appears to be the best catalyst, owing to its high activity at low temperatures.(Mariño *et al.*, 2004)

Gold-based catalysts are also regarded as efficient catalysts for CO oxidation and several experiments are performed with Au/TiO_2 and $Au/\alpha\text{-}Fe_2O_3$. The influence of H_2 in the feed is examined with Au/TiO_2 catalyst and higher CO reaction order is obtained in the presence of H_2 (Schumacher *et al.*, 2004). The effect of CO_2 addition is also investigated, and the results obtained show that it decreases the CO oxidation rate; whereas, water addition increases the selectivity by suppressing H_2 oxidation reaction. The study also showed that the extent of water addition depends on the reaction temperature. According to another study, gold-based catalysts show resistance to deactivation by water and carbon dioxide addition (Trimm, 2005). Mariño *et al.* compare the activities and selectivities of different catalysts, and reached the result that Au catalysts deactive much rapidly than Pt catalysts (Mariño *et al.*, 2004).

As an alternative to the supported noble metal catalysts for PROX, CuO/CeO_2 catalysts show high activity and selectivity, due to the low value of activation energy of CO oxidation over CuO/CeO_2 system. Caputo *et al.* concluded that the reaction kinetics is highly influenced by reaction temperature, whereas it is weakly affected by CO_2 and H_2O concentration (Caputo *et al.*, 2007). The kinetic study of CO oxidation over CuO/CeO_2 was also carried out and consistent orders and activation energy with the literature were obtained (Moreño *et al.*, 2008).

Regarding the previous research over Pt-based catalysts, PROX reaction kinetics was also studied over Pt catalyst and the convenience of the Pt-surface has been examined (Bissett *et al.*, 2005). $Pt/\gamma\text{-}Al_2O_3$ was used in order to study the effect of particle size on PROX reaction rate and selectivity. The experiments were performed while λ ($\lambda=2P_{O2}/P_{CO}$) was fixed to 1. Based on the experiments, larger particle sizes contribute to higher turnover rates. The increase in oxygen partial pressure leads to an increase in reaction rate, implying that oxygen partial pressure dependency on reaction kinetics are rather high on larger particles (Atalik *et al.*, 2006).

Alumina-supported Pt-, Rh-, Ru-, Au-catalysts were examined for preferential CO oxidation by Kipnis *et al.* The results of the experiments over all the catalysts have indicated that carbon monoxide can show deactivating effect over Pt-, Rh-catalysts during preferential oxidation of CO due to its strong adsorption over these metals, even in the presence of hydrogen (Kipnis *et al.*, 2010).

CeO_2 is an alternative support to alumina for Pt-based catalysts. Research carried out by Polster *et al.* uses Pt/CeO_2 catalyst for preferential CO oxidation. In their work, different Pt loadings and dispersions over a series of Pt/CeO_2 catalysts were tested for the reactions of CO and H_2 oxidation. Dual Langmuir–Hinshelwood (L–H) and Mars and van Krevelen (M–vK) pathways were studied in the mechanistic analyze and to examine the loss in CO oxidation selectivity at low CO concentrations as well. The conclusions attained from this study confirm that at low CO coverage, Langmuir–Hinshelwood kinetics dominates, whereas at high CO coverage the situation is reversed. In addition to this, low gas phase CO coverage on Pt leads to selectivity losses at low CO concentrations (Polster *et al.*, 2010). The same catalyst was also evaluated by Ayastuy *et al.* and showed high activity and selectivity for preferential CO oxidation even at low temperatures, which minimizes hydrogen oxidation selectivity. Addition of CO_2 in the feed stream activates the catalyst slightly, whereas water addition inhibits the catalytic activity. The presence of CO_2 and H_2O in the feed stream showed these effects especially at higher temperatures (Ayastuy *et al.*, 2006).

2.5.2. Metal Oxide Supported Bimetallic PROX Catalysts

According to the research performed with different catalysts including various materials and supports, base metal added Pt-based catalysts showed superior ability for the removal of CO. Base metals addition such as Co, Ni or Mn was shown enhances the performance of Pt/Al_2O_3 catalytic activity and optimum reaction conditions were obtained for $Pt\text{-}Co/Al_2O_3$ (Suh *et al.*, 2005). Another study that investigates Pt catalysts promoted by Co and also K, is published by D.L.Trimm and it is projected as the best catalyst for selective CO oxidation (Trimm, 2005).

Pt-Co-Ce/Al_2O_3 catalyst was also used in another study. The goal was to obtain an effluent with a CO concentration of less than 10 ppm with a high selectivity (77%) to the selective CO oxidation. According to the results, CO-PROX reaction was enhanced at low temperatures and with the presence of CO_2 in the inlet gas. On the contrary, H_2O showed a negative influence. The oxygen excess indicated opposite effects on CO conversion and oxygen selectivity to CO_2 (Lobera *et al.*, 2010).

Bimetallic carbon supported Pt-Sn catalysts showed superior performance relative to commercial Pt-Al_2O_3 catalysts regarding their high activity and selectivity at low temperatures. These catalysts have been studied kinetically for preferential oxidation of CO; there the effect of H_2 on kinetic parameters was investigated as well (PROX). Selectivity is extremely high at low temperatures (85%) in the range 0-20^{0}C. Though selectivity decreases with temperature, it is still higher (45%) at 120^{0}C compared to the standard Pt catalysts. The decrease of selectivity with increasing temperature by bifunctional surface was explained by the competition between CO and hydrogen for Pt sites. By means of temperature programmed desorption (TPD), in situ diffuse reflectance IR Fourier transform spectroscopy (DRIFTS), and x-ray photon spectroscopy (XPS) measurements, it is concluded that surface coverage of CO on metallic particles is high and reduction occurs only in some part of Sn in Pt-Sn alloy particles (Schubert *et al.*, 2001).

Preferential oxidation of CO was studied in the presence of H_2 with monometallic Pt/γ- Al_2O_3, bimetallic PtSn/γ- Al_2O_3 and also a K or Ba modified PtSn/γ- Al_2O_3. Sn/Pt ratio used in the experiments was 1.6. Pt-Sn-K/γ- Al_2O_3 showed the maximum activity and selectivity among all the catalysts. Another result reached at the end of these experiments was that the activity of the catalysts increase with tin addition, and since CO-Pt interactions are weakened this leads the reaction to occur at lower temperatures. The selectivity of the CO oxidation relative to H_2 oxidation increases with the addition of K or Ba. The selectivity passes through a maximum as a function of temperature, which is led by the equilibrium nature of reverse WGS, which is the side reaction, especially for low CO concentration levels. As a result, in order to avoid the negative influences of RWGS using low temperatures during reaction should be preferred (Siri *et al.*, 2007).

Another study focuses on the effects of CO_2-H_2O in the feed stream and temperature on PROX. In the study, a Pt–SnO_2/Al_2O_3 sol–gel catalyst, that had been previously designed for the reaction feed free from CO_2 and H_2O, was used. In the absence of CO_2 and H_2O, 100% CO conversion was reached at 110^0C with 1% CO, 1% O_2, 58% H_2 and helium as balance in the feed stream. CO conversion fell down to 47% by the addition of CO_2 in the feed, however contribution of 10% H_2O, pulled the conversion level back to 100%. The results obtained at 120^0C and 130^0C showed that the activity loss was increased with temperature (Uysal *et al.*, 2006).

2.6. Catalyst Supports

The reactivity of heterogeneous catalysts stems from the active surface centers. Consequently great effort is made to maximize the effective surface area (i.e. metal surface area or dispersion) of a catalyst by distributing its active metal(s) over a high surface area support. Special interest is shown on support catalysts since they allow to reach dispersion and stabilization small metallic particles as well. The support may be inert or participate in the catalytic reactions. Besides its high surface area, a catalyst support should have high porosity and has low cost. Typical supports include various kinds of carbon, alumina, and silica. In fuel cells, platinum catalysts are located on a carbon support, which provides a means for conduction of the electrons for the electrocatalytic reactions.

2.6.1. Activated Carbon

The most important factors that determine the properties and performance specs of activated carbons are surface area, porosity, pore volume distribution, and surface chemical composition. Activated carbon is a very porous material; its surface area most of the time well above 500 m^2/g. Its surface makeup is described as sponge-like, riveted with microscopic holes and crevices similar to sandpaper. The physical structure of activated carbon is only viewable with a microscope, due to the small sizes of its holes and rivets. Activated carbon may appear smooth and granite-like when it is observed by the naked eye.

Figure 2.3. Schematic representation of the structure of activated carbon.

Besides its high surface area and porosity, activated carbon has a unique property; its surface chemistry can be modified according to the targeted adsorbent/support properties. As the oxygen bearing surface groups of activated carbon form anchoring sites for the metal precursors in catalyst preparation through modifying the type and abundance of these surface groups one can modify dispersion of metallic phases and even may help the formation of beneficial alloys during the preparation and treatment of bimetallic catalysts.

In the fine chemical industry catalysts based on precious metals on activated carbon supports are frequently used, because such systems exhibit interesting features with regard to their application. Contrary to the alumina and silica, activated carbon is stable in both acidic and basic media (Auer *et al.*, 1998).

Activated carbons formed must also exhibit sufficient high crush strength. Together with the surface chemistry of the activated carbon, these factors strongly influence the performance of the activated carbon supported catalysts.

L.Wang *et al.* found that the activated carbon with enriched oxygen-containing groups and macropore structure played an important role in CO catalytic oxidation (Wang

et al., 2010). Platinum on activated carbon support is also the most frequently used catalyst to build up the anode and the cathode side in PEMFC (Auer *et al.*, 1998).

There are mainly seven types of surface groups can be formed on the activated carbon surface, including carboxylic acid, lactone, phenol, carbonyl, anhydride, ether and quinone groups. The acidic or basic behavior and the redox properties of activated carbon is based on these functional groups.

The acidic groups on the surface decrease the hydrophobicity of the carbon, leading to the accessibility of the surface to aqueous metal precursors, while the less acidic groups increase the interaction of the metal precursor or the metal particle with the support and, as a consequence, minimize the sintering propensity of the metal on carbon (Aksoylu *et al.*, 2000a).

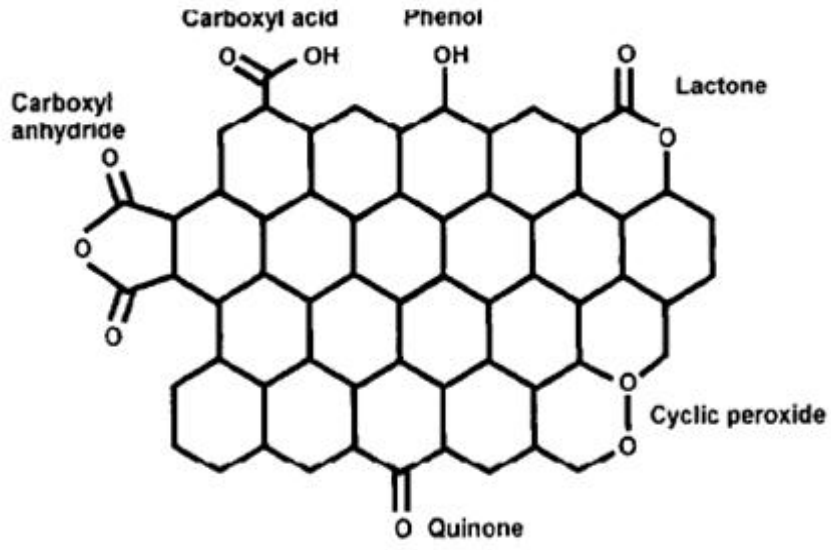

Figure 2.4. Some types of oxygen surface groups in activated carbon.

2.6.2. AC Based PROX Catalysts

The effects of different types of activated carbon supports and support modifications on the properties of Pt/AC catalysts were investigated by Aksoylu *et al.*. Air oxidation and HNO_3 oxidation treatment have prominent effects on the chemical properties

of activated carbon, however effects on textural properties are rather limited. They differ in the case that air oxidation results with formation of basic type surface oxygen bearing groups, which are stable during high temperature catalyst pretreatments like calcinations, whereas HNO_3 oxidation leads to large number of carboxylic groups which can decompose comparably lower temperatures. Both oxidation treatments enhance the dispersion of Pt metallic crystallites. (Aksoylu *et al.*, 2001).

The selective oxidation of CO in a H_2 rich gas stream was studied over a series of Pt-Ce and Pt-Sn catalysts supported on activated carbon. Three types of activated carbon were used: (i) grinded and HCl washed activated carbon, (ii) air-oxidized form of the first one , and (iii) HNO_3 oxidized form of the first one. The experimental results showed that, oxidized AC samples, especially HNO_3-oxidized AC enhances Pt–CeO_x and Pt–SnO_x interaction and alloy formation The highest activity and selectivity was obtained with Pt-Sn catalyst on air-oxidized AC among all the combinations (Özkara *et al.*, 2003).

Additional study was performed to compare the performances of 1% Pt–0.25% SnO_x and 1% Pt–1% CeO_x catalysts supported on non-oxidized and oxidized activated carbon (AC) in H_2-rich gas streams containing CO_2 and H_2O. Addition of CO_2 and H_2O was examined for nine different activated carbon supports with feed mixtures containing 1% CO, 1% O_2, 60% H_2 and He. It was found that, the addition of CO_2 resulted with an increase of CO conversion surprisingly for all the catalysts supported on oxidized or non-oxidized AC. 100% CO conversion was achieved with1% Pt–0.25% SnO_x supported on the HNO_3-oxidized activated carbon support, in the presence of CO_2 and/or (CO_2 + H_2O) in the feed (Şimşek *et al.*, 2007).

A detailed study on Pt-Sn/AC CO oxidation catalysts, which prepared by coimpregnation method and sequential impregnation method was conducted. The results indicated the pronounced changes in catalytic properties depending on the abundance of surface oxide groups of the supports and Pt-Sn interaction. Justifying the results in the article published by Aksoylu *et al.* in 2001, oxidation treatment on AC and introducing Sn as the second metallic phase prevent the mobility of surface Pt during reduction. HNO_3 oxidation pretreatment creates an acidic surface having less thermally stable carboxylic acid groups, which helps the formation of Pt-Sn alloys, especially Pt-rich Pt_3Sn. The

comparison of the catalytic properties of the catalysts prepared by different impregnation methods revealed that sequentially impregnated catalysts in which Sn is introduced first, have higher adsorption capacities than coimpregnated ones. Among all the tested catalysts, 1wt% Pt- 0.25wt % Sn/AC prepared by sequential impregnation on the HNO_3 oxidized support, showed the highest activity and reached 100% CO conversion (Aksoylu *et al.*, 2000b).

2.7. Kinetics of PROX Reaction

There are numerous studies about PROX kinetics under ideal conditions, i.e. for the feed stream consists of CO, O_2 and inert. However, a kinetic study on CO oxidation under realistic conditions has been rarely studied. It is very valuable to perform kinetic tests aiming to obtain a power-law type rate expression for CO oxidation under the flow of feed mixture having composition same as the LTS reactor effluent of a typical fuel processor. Since downstream of WGS reactor carries CO, O_2, CO_2, H_2, CH_4, H_2O, kinetic study under realistic conditions should include these gases in the feed stream. Low temperatures (100^0C-130^0C) are preferred in these studies, due to the enhancement of H_2 oxidation at higher temperatures. The effect of presence of CO_2, H_2, etc. was examined individually or in combination, but kinetic expression that takes all into account, could not be found though it is essential for the realistic design of the PROX reactor.

PROX kinetics at low temperatures was studied over 1wt% Pt-1wt%CeO_x/AC oxidized by air and a power model rate expression is obtained with negative dependence on CO (-0.24) and positive dependence on O_2 (0.98) under ideal conditions, i.e. with feed having CO, O_2, and inert. Besides the rate expression, the effects of the presence of additional CO_2 and H_2 in the feed stream were also examined. Addition of CO_2 resulted with a decrease in CO conversion as expected and the selectivity of CO oxidation reaction decreases with increasing amounts of H_2 in the feed (Gülyüz *et al.*, 2009).

Low temperature CO oxidation kinetics was also studied over 1% Pt–0.25% SnO_x supported on the HNO_3-oxidized activated carbon support) using various concentrations of CO (1-10 mol%) and O_2 (1-4 mol%). Reaction rate was expressed as power-function with positive dependence on CO (0.96) and negative dependence on oxygen (–0.31) in the

absence of H_2. The CO oxidation rates reached 10 times higher values at H_2 concentrations above 30 mol% where the CO oxidation selectivity is 46% (Baltacıoğlu *et al.*, 2007).

3. EXPERIMENTAL WORK

The flow diagram of experimental work within the scope of the current study is presented below (Figure 3.1).

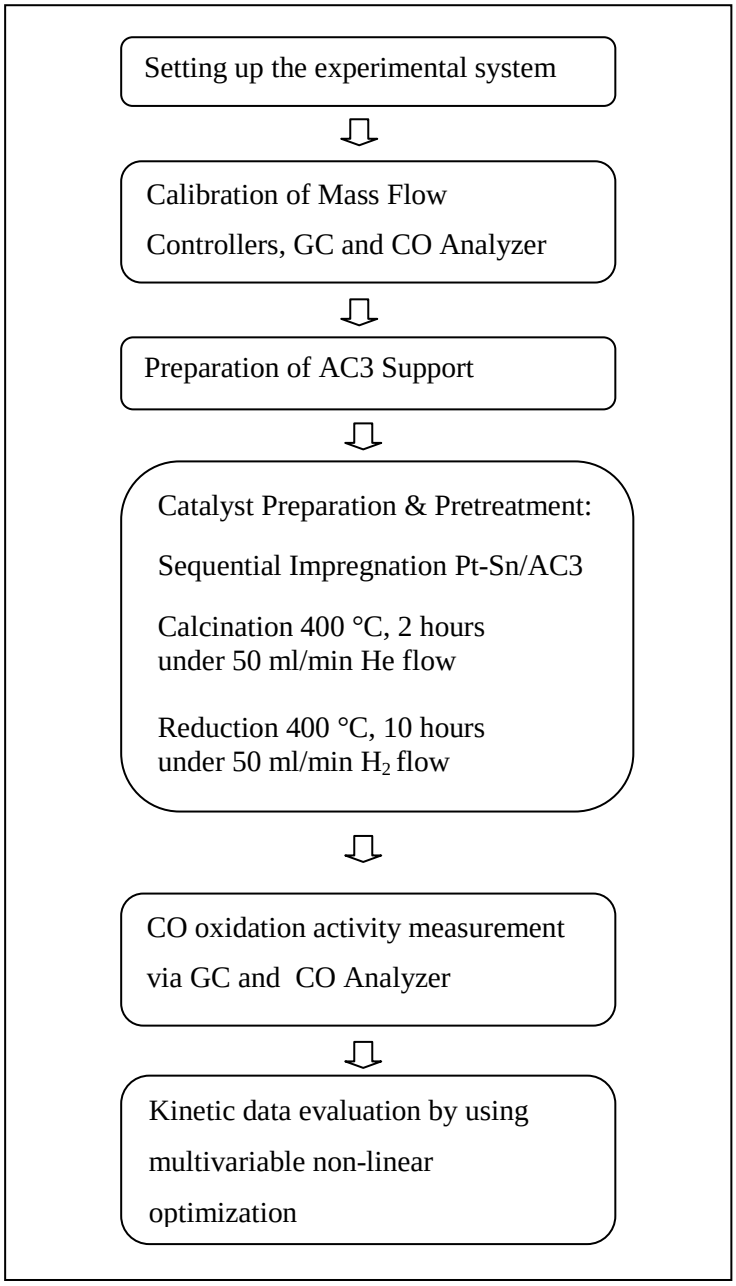

Figure 3.1. A Schematic diagram of the experimental work done in this study.

3.1. Materials

3.1.1. Chemicals

The catalysts that were tested in this study were prepared based on the previous study performed by Aksoylu (Aksoylu *et al.*, 2000b). The chemicals used for catalyst preparation are listed in Table 3.1.

Table 3.1. Chemicals used in catalyst preparation.

Chemicals	**Formula**	**Grade**	**Source**	**Molecular Weight (g/mole)**
Hexachloroplatinic(IV)acid Hexahydrate	$H_2PtCl_6.6H_2O$	Extra pure	Merck	517.9
Tin(IV)chloride	$SnCl_4.5H_2O$	Extra pure	Riedel-de Haën	350.5
Activated carbon	C	ROX 0.8	NORIT	12
Nitric Acid	HNO_3	Research	Merck	63.0
Hydrochloric acid	HCl	Research	Merck	36.5

3.1.2. Gases and Liquids Used

All of the gases used in this study were supplied by BOS (Birlesik Oksijen Sanayii) Company, Istanbul, Turkey. Table 3.2 gives the specifications and the use of these gases.

Table 3.2. Specifications and applications of the gases and standards used.

Gas/Standard	**Specification**	**Application**
Carbon monoxide	99.999% BOS	GC calibration, Reactant
Oxygen	99.999% BOS	GC calibration, Reactant
Carbon dioxide	99.999% BOS	Reactant
Helium	99.99% BOS	Reactant
Methane	99.99% BOS	Reactant
Hydrogen	99.99% BOS	Reactant, reducing agent
Helium	99.99% BOS	GC carrier
Dry Air	78.4 % N_2 + 21.5 % O_2 (BOS)	GC calibration, CO Anayzer calibration

Table 3.3. Specifications and applications of the liquids used.

Liquid	**Specification**	**Application**
Water	Distilled	Aqueous solutions, Reactant

3.2. The Experimental Set-Up

The experimental set-up consists of the following systems:

(i) AC preparation system which was used for the preparation of HNO_3 – oxidized AC support

(ii) Catalyst preparation system which was used in the preparation of sequentially impregnated Pt-Sn/AC3 catalysts

(iii) Reaction test system which was used in the PROX kinetics tests over Pt-Sn/AC. The reaction test system includes three sub units, namely reactant stream preparation unit, temperature controlled reactor and the analysis block including a CO analyzer and a GC.

3.2.1. Catalyst Preparation System

The system used for catalyst preparation by sequential impregnation technique includes a Retsch UR1 ultrasonic mixer, a vacuum pump, a buchner flask and a MasterFlex computerized-drive peristaltic pump.

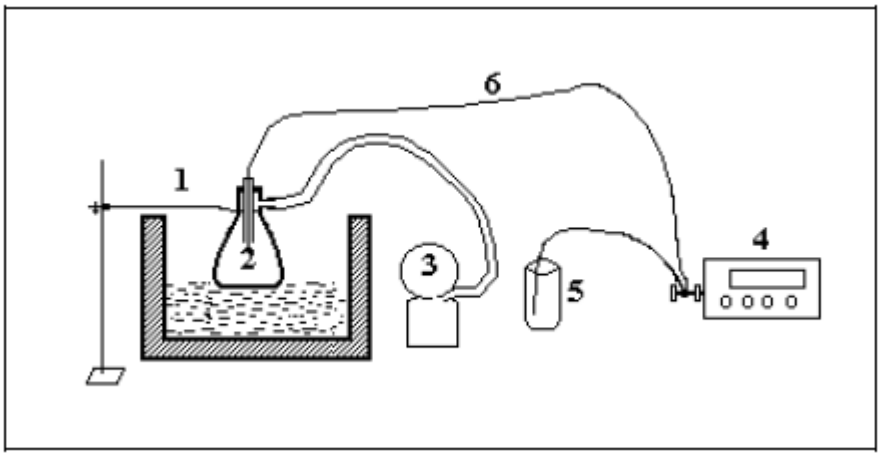

Figure 3.2. The impregnation system: 1. Ultrasonic mixer 2. Vacuum flask 3. Vacuum pump 4. Peristaltic pump 5. Beaker 6. Silicone Tubing (Akın, 1996).

3.2.2. Catalytic Reaction System

The catalytic reaction system designed and constructed in CATREL has three sections:

- Feed section
- Reaction section
- Product analysis section

The feed section includes mass flow control systems, 1/4", 1/8" and 1/16" stainless steel tubes and fittings for feeding liquid water and gaseous species, i.e. oxygen, hydrogen, carbon monoxide, carbon dioxide, methane, helium and dry air at desired quantities. The gases that were present in pressurized cylinders were passed through the gas flow regulators and the calibrated Brooks mass flow controllers. Two Brooks CC1A10 series control boxes are used to regulate the gas flows. On-off valves were placed in front of the mass flow controllers to protect them from possible back-pressure fluctuations. All the reactants excluding water were then passed through a primary mixing zone to ensure the flow of a homogeneous gas mixture into the reactor.

Water was introduced into the reaction system at constant flow rates using Agilent 1200 series HPLC pump. The 1/16" tube, through which water was allowed to flow was kept at 423 ± 3 K by a 1.4 m heating tape whose temperature is controlled by PID-type temperature controller to feed water in the form of steam. Steam and the homogeneous gas mixture were mixed in a secondary mixing zone**.**

It was possible to divert flow by using a transfer line having three way valves: The feed gases could be diverted to the bypass line, so that feed composition could be analyzed using the gas chromatograph and/or CO analyzer. Another three way valve was used for diverting the flow to the bypass vent line for establishing steady state flow and mixing of the steam and other gaseous reactants prior to the reaction.

The reactants, metered and mixed in the feed section, were allowed to flow through the reaction section. This section was composed of a 50 cm x 2.4 cm ID tube vertical

oven whose temperature is controlled to ± 0.5 K by Eurotherm 3216 programmable temperature controller and a 1/4" stainless steel fixed-bed microreactor placed inside the oven. The reactor was also constructed in CATREL and its length was selected to be 60 cm so that it was longer than the furnace.

During the reaction tests, the catalyst bed was placed at the center of the reactor. The reaction temperature was measured by a 20-gauge wire K type sheathed thermocouple (insulation material: ceramic fiber braid) that was placed in the center of the furnace. The thermocouple is connected to the temperature controller supplying feedback data for controlling the reactor oven temperature. The position of the reactor and hence catalyst bed was adjusted to coincide with the constant-temperature zone of tube furnace. Silane-treated glass wool (Alltech Associates Inc.) was used to hold the catalyst bed in a fixed position. Ceramic glass wool insulations were placed in top and bottom ends of the reactor furnace to prevent heat loss from the furnace and to provide a good temperature profile.

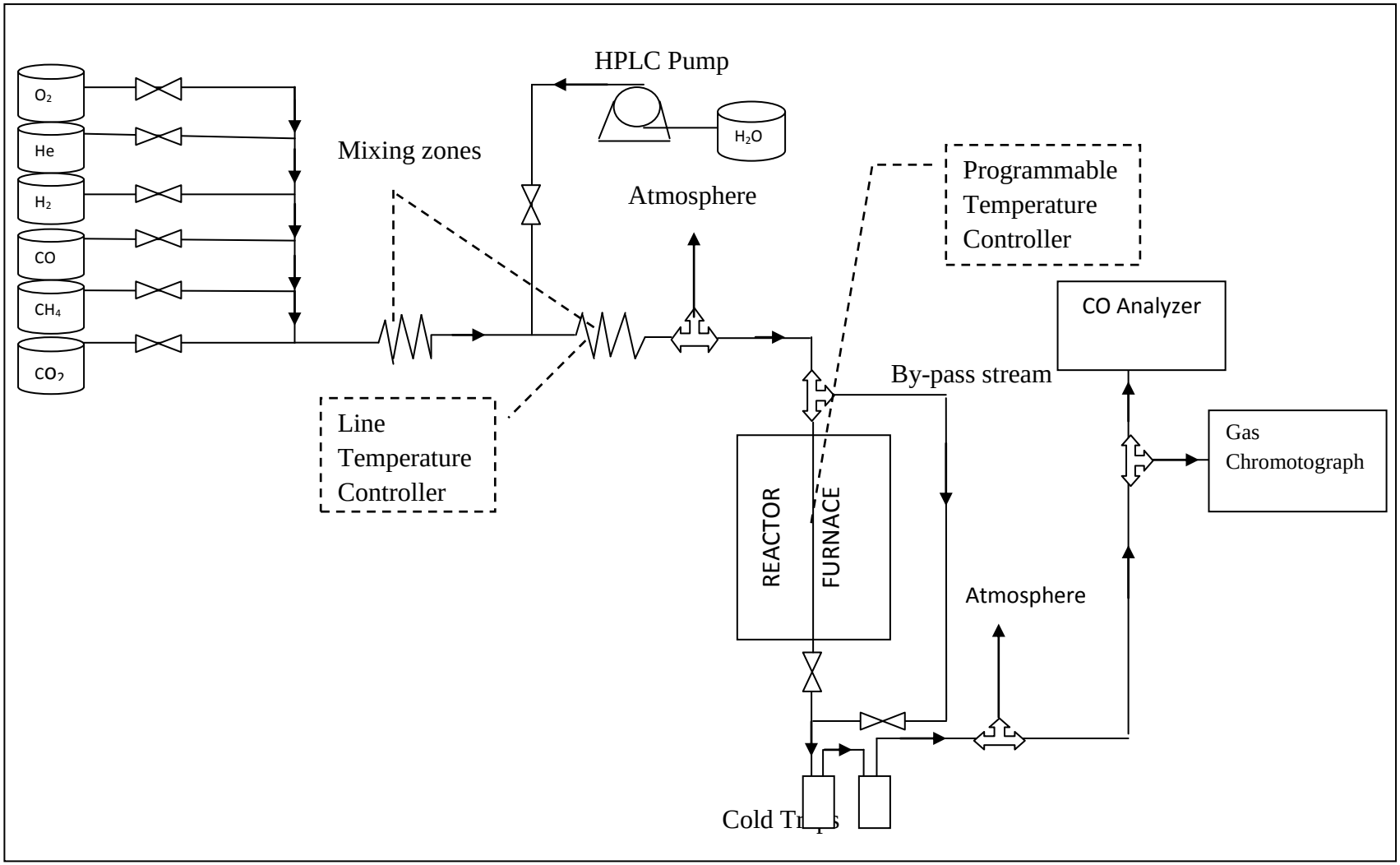

Figure 3.3. Flowsheet of the microreactor system.

3.2.3. Product Analysis Systems

Preferential CO oxidation has a side reaction, which is hydrogen oxidation namely. Hence the product stream needs to be analyzed not only in terms of carbon monoxide, but also in terms of oxygen concentration. CO concentration data is obtained from Thermo Electron Corporation Model 48i CO Analyzer, while O_2 concentration data is obtained from Agilent Technologies 6850 Series II Gas Chromotograph.

CO analyzer operates on the principle that CO absorbs infrared radiation at a wavelength of 4.6 microns. Infrared absorption is a non linear measurement technique therefore, it is necessary to transform the basic analyzer signal into a linear output. The CO analyzer uses and internally stored calibration curve to accurately linearize the instrument. This calibration curve limits the CO analyzers upper concentration range to 10000 ppm.

The experiments were conducted within the range of 10-1000 ppm, which is well below the upper limit (Table 3.4). The operation diagram of the CO analyzer is given in Figure 3.4. The sample flows through an optical bench. Radiation from an infrared source is chopped then passed through a gas filter alternating between CO and N_2. The radiation then passes through a narrow bandpasss interference filter and enters the optical bench where absorption by the sample gas occurs. The infrared radiation then exits the optical bench and falls on an infrared detector. The CO gas filter acts to produce a reference beam which cannot further be attenuated by CO in the sample cell. The N_2 side of the filter wheel is transparent to the infrared radiation and therefore produces a measurement beam which can be absorbed by CO in the cell. The chopped detector signal is modulated by the alternation between the two gas filters with an amplitude related to the concentration of CO in the sample cell. Other gases do not cause modulation of the detector signal since they absorb and measure beams equally. Therefore the system responds specifically to CO.

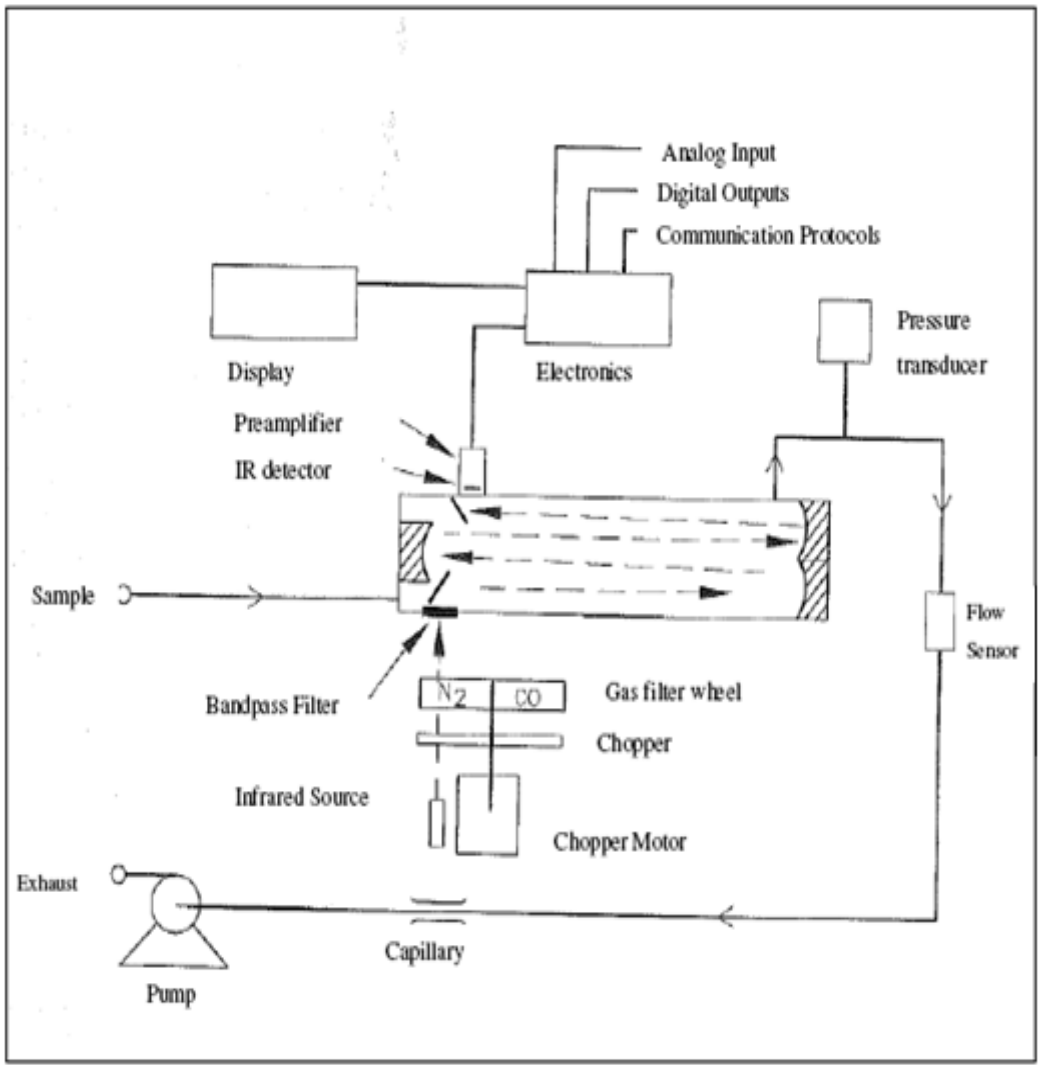

Figure 3.4. Schematic of the CO Analyzer (Soykal, 2006).

Agilent 6850C equipped with a Thermal Conductivity Detector (TCD) is used to analyze the product gas. An Alltech CTR1 column with the outer packing material of 6ft x 1/4" Packed with Activated Molecular Sieve and with the inner packing material of 6ft x 1/8” porous polymer mixture. Analysis conditions are given below in Table 3.5.

Table 3.4. CO analyzer specifications.

Range	0-1 to 10000 ppm
Zero Roise	0.02 ppm RMS (30 second averaging time)
Lower Detectable Limit	0.04 ppm
Zero Drift	<0.1 ppm
Span Drift	±1 % full-scale
Response Time	60 seconds (30 second averaging time)
Linearity	±1% of full-scale ≤1000 ppm
	±2.5% of full-scale > 1000 ppm
Sample Flow Rate	1.0 LPM
Operating Temperature	20- 30°C (may be safely operated over the range of 0-45°C)

Table 3.5. Reactant and product gas analysis conditions.

Column Type	CTR I (Packed Concentric Column)
Outer Column Packing	Activated Molecular Sieve
Inner Column Packing	Porous Polymer Mixture
Column Oven Temperature	353 K
Carrier Gas	Helium
Carrier Gas Flow Rate	20 ml/min
Detector Type	Thermal Conductivity
Detector Current	120 mA
Front Detector Temperature	493 K
Front Inlet Temperature	393 K
Auxillary Temperature	323 K

3.3. Catalyst Preparation

The activated carbon supported catalysts were prepared by incipient wetness impregnation method previously used by Özkara (2003). The catalysts prepared by impregnation method. 1% Pt- 0.25% Sn over Activated Carbon 3 (HNO_3 oxidized AC) catalyst was used for experiments.

3.3.1. Pretreatment of the AC Support

Commercial activated carbon (AC) kindly supplied by NORIT (NORIT ROX) was crushed and sieved into 45–60 mesh size (344–255 μm) and exposed to different thermal and chemical pretreatments indicated below prior to being used as supports.

• Firstly, activated carbon material was treated with 200 ml of 2 N HCl of 200 ml acid solution to remove some ash content and Sulfur accompanied with it. This treatment was carried out in a Soxhlet apparatus. Approximately 15 g of commercial activated carbon was placed in an extraction unit held by a cellulosic cup. Extraction process was continued under reflux for 12 hours. The slurry was then rinsed with 250 ml distilled water and washed again for 6 hours inside the Soxhlet apparatus to remove HCl remaining on the support surface. Finally, the slurry was dried at 115°C overnight. This support is called AC1.

• AC1 support was oxidized in a down flow reactor, heating it from room temperature up to 450°C under the flow of 15 ml/min N_2 with 10°C/min heating rate. It was kept at 450°C under the flow of 150 ml/min N_2-50 ml/min dry air mixture for 10 hours and was cooled down to room temperature under the flow of 150 ml/min N_2. This procedure gave the second type of AC support called AC2. AC2 catalysts were not used in this work.

• 15 g of AC1 was put into a round bottom flask containing 350 ml of 5 N HNO_3 solution. This flask was heated up under total reflux for 3 hours. Afterwards, the oxidized sample was rinsed with boiling distilled water for 2 hours. The rinsing procedure was repeated 3 times, and then the slurry was dried at 115°C overnight. The third type of AC support thus obtained is called AC3.

3.3.2. Impregnation

The experimental set-up shown in Figure 3.2 was used for catalyst preparation by the incipient to wetness impregnation. Incipient wetness impregnation method that was used in the study consists of three parts:

- Evacuating the support,
- Contacting the support with the precursor solution, and
- Drying.

For incipient to wetness impregnation, five grams of activated carbon was placed in the vacuum flask and kept under vacuum both before, during and after the addition of precursor solutions. Since trapped air in the pores of the support could prevent penetration of the solutions, vacuum pump was used to remove the trapped air and to give a uniform distribution of the active component. Before impregnating the solution, the support material was mixed with ultrasonic mixer for 25 min.

A Masterflex computerized-drive peristaltic pump was used to feed the precursor solution to the vacuum flask at a rate of 0.5 mL/min via slicone tubing. The slurry was mixed by an ultrasound mixer during the impregnation in order to maintain uniform distribution of the precursor solutions. After the precursor solution was added, the slurry was ultrasonially mixed for additional 90 min. The thick slurry obtained was dried at 115°C overnight.

3.4. Selective CO Oxidation

3.4.1. Catalyst Activation

The results obtained from the study conducted by Özkara (2003) showed that reduction at 673 K results in densely populated active sites placed very close to each other. Here, reduction temperature for Pt-Sn/AC3 catalyst was also chosen as 673 K. The activated carbon supported catalyst was calcined in situ under He with flow rate of 50 ml/min at 673 K for 2 hours and then reduced by H_2 with flow rate of 50 ml/min for 10

hours prior to the reactions. The reduction time length is obtained from the study of Aksoylu (2000b) Temperature procedure is given in Table 3.6.

Table 3.6. Temperature program for the in situ pretreatment activated carbon supported catalysts.

Segments	**Starting and End Temperatures**	**Segment Gas**
First	Heating from 293 K to 393 K with a heating rate of 10 K/min	He with flow rate of 50 ml/min
Second	Keeping constant at 393 K for 10 min	He with flow rate of 50 ml/min
Third	Heating from 393 K to 573 K with heating rate of 10 K/min	He with flow rate of 50 ml/min
Fourth	Heating from 573 K to 673 K with a heating rate of 10 K/min	He with flow rate of 50 ml/min
Fifth (Calcination)	Keeping constant at 673 K for 2 hrs	He with flow rate of 50 ml/min
Sixth (Reduction)	Keeping constant at 673 K for 10 hrs	H_2 with flow rate of 50 ml/min
Seventh	Sweeping at 673 K for 1 hrs	He with flow rate of 50 ml/min

3.4.2. PROX Reaction Kinetic Experiments

All the reactions were conducted in the micro reactor system whose flow sheet is presented in Figure 3.2. The total flow rate is kept constant at 100 ml/min. CO oxidation was studied under atmospheric pressure at a temperature of 110^0C. The weight of the catalyst was 20 mg in the first set of experiments and 15 mg in the second set. Hence the ratio "weight of the catalyst over the flow rate" (W/F) was varied in order to obtain the activity data for to be used in linear fit plot in order to obtain the initial rates data. The ratio of oxygen to carbondioxide is taken 1, 1.25, 1.5, 2, 2.5, 3 in the experiments. The flowrates of hydrogen, carbondioxide, methane and water were kept constant as 60%, 15% and 3%

respectively, while carbonmonoxide and oxygen flow rates were changed in the range of 1-2.5% and 1-1.5% respectively aiming to analyze the effect of CO and O_2 concentration in the feed on the activity level achieved. During the experiments, the flow of helium was changed to compensate the parametric changes in CO and O_2 flows in order to fix the total volumetric flow of the feed at 100 ml/min.

Table 3.7. Reaction conditions.

Parameter	**Value**
Catalyst Particle Size (mesh size)	45-60 (344-255μm)
Catalyst Amount (mg)	15- 20
Reduction Temperature (^oC)	400
Reaction Temperature (^oC)	110
Reaction Total Flow Rate ($ml.min^{-1}$)	100

After the catalyst preparation step, the catalyst was isolated in pure helium (inert) atmosphere and the feed gases were sent through the bypass line. Thus the feed gases would not start to react before the flow reaches steady state. The CO analyzer collects real time data, therefore steady state was assumed to be achieved after the CO readings stay constant for more than 5 minutes. The CO analyzer is designed to work in an open atmosphere and therefore it is calibrated according to the laboratory's ambient atmosphere. The trace amount of CO from the atmosphere is the base set value for the CO analyzer. Notice that between summer and winter months the CO content in the atmosphere changes due to heating issues; however, the base line is observed to change by only 50 pbm. Thus, it is safe to neglect the trace amount of CO in the air. The inlet flow rate of the CO analyzer was 1.089 ml/min. The make - up stream of the CO analyzer was provided by dry air from the high purity cylinder. The CO analyzer readings, which do not reflect the exact concentration of CO in the feed stream due to dilution with air, were corrected accordingly for finding the CO concentration in the reactor exit. Refer to Figure 3.4 for the block diagram of the CO analyzer and Eqn 3.1 for the CO concentration in the feed.

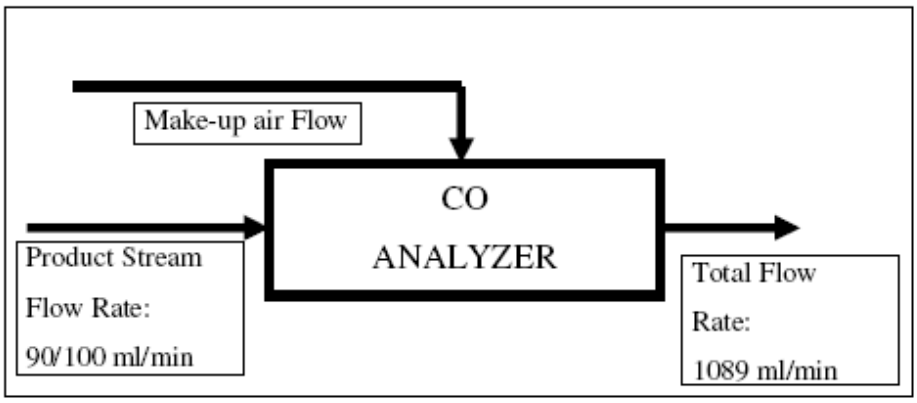

Figure 3.5. Block diagram for the CO analyzer.

$$CO\,in\,the\;\;product\;\;stream = \frac{What\,is\;\;read\;\;on\;\;CO\;Analyzer \times 1089}{100} \tag{3.1}$$

Table 3.8. A summary of the experimental conditions for the 1%Pt-0.25%Sn/AC3 catalyst.

Exp	**T (^{0}C)**	**W_{cat} (mg)**	**O:CO ratio**	**CO flow rate (ml/min)**	**O_2 flow rate (ml/min)**	**H_2 flow rate (ml/min)**	**CO_2 flow rate (ml/min)**	**CH_4 flow rate (ml/min)**	**H_2O flow rate (ml/min)**	**He flow rate (ml/min)**
1	110	20	2	1	1	60	15	3	10	10
2	110	20	2.5	1	1.25	60	15	3	10	9.75
3	110	20	3	1	1.5	60	15	3	10	9.5
4	110	20	2	1.25	1.25	60	15	3	10	9.5
5	110	20	1	2	1	60	15	3	10	9
6	110	20	1.5	2	1.5	60	15	3	10	8.5
7	110	20	1	2.5	1.25	60	15	3	10	8.25
8	110	15	2	1	1	60	15	3	10	10
9	110	15	2.5	1	1.25	60	15	3	10	9.75
10	110	15	3	1	1.5	60	15	3	10	9.5
11	110	15	2	1.25	1.25	60	15	3	10	9.5
12	110	15	1	2	1	60	15	3	10	9
13	110	15	1.5	2	1.5	60	15	3	10	8.5
14	110	15	1	2.5	1.25	60	15	3	10	8.25

4. RESULTS AND DISCUSSION

4.1. Introduction

The goal of this study is to obtain a power-law model rate expression for preferential CO oxidation over 1% Pt-0.25% Sn/AC3 under fully realistic reaction conditions. In the experiments residence time (W_{cat}/F_{CO}), oxygen concentration and carbonmonoxide concentration in the feed stream were changed parametrically while hydrogen, carbondioxide, methane and water vapor concentrations were kept constant. As the power-type rate expression was aimed to be established in terms of CO and O_2 concentrations, initial rate data for each predetermined CO and O_2 concentration combination were obtained by varying W_{cat}/F_{CO} through changing catalyst weight while keeping all other parameters constant.

In the activated carbon support preparation procedure, nitric acid treatment was applied in order to increase the amount of oxygen bearing groups, specifically carboxylic groups, on the support surface. The catalysts were prepared by sequential impregnation for which Sn precursor was impregnated first. This sequence enables formation of alloy between Pt and Sn, especially Pt_3Sn; our previous results confirm the presence of well dispersed Pt_3Sn and Pt sites on the catalyst surface.

Preferential CO oxidation kinetics under ideal conditions was studied by many researchers. In this study PROX kinetics data were obtained under realistic conditions, in which CO_2, H_2O, CH_4 also exists in the feed stream. A temperature of 383 K was selected for intrinsic rates region using CO concentrations between 1% and 2.5% at various O:CO ratios (λ=1-3) and space times (W_{cat}/F_{CO}= 0.0147 - 0.0489 mg min μmol^{-1}). Two set of experiments were performed. First set consist 7 experiments with varying CO and O_2 concentrations in the feed and were carried out over 20 mg 1% Pt- 0.25% Sn/AC catalyst. In the second set 7 experiments were repeated with 15 mg catalyst. CO conversion levels were determined from data collected by Thermo CO Analyzer, while O_2 conversion were determined by using data collected by Agilent Technologies 6850 Series II Gas Chromotograph.

4.2. Catalysts Characterization

Reduction procedure applied is one of the most important parameter that predominantly determines the properties and performance of Pt-Sn system supported on nitric acid oxidized activated carbon (AC3). It affects the interaction between metal precursors allowing alloy formation (Özkara and Aksoylu, 2003). The calcination and reduction temperature was selected to be 400^0C, which enables formation, dispersion, and stability of the active centers on the catalyst. Considering the fact that AC3 was used as the support, calcination step was performed under He flow. During calcination procedure, the temperature was first raised to 125^0C and the temperature was kept fixed at that level for 20 minutes aiming to remove water residues in the pores. The temperature was raised to 300^0C, kept fixed at this level for 20 minutes and then was raised to the calcination temperature 400^0C, and kept fixed at that level for 2 hours to stabilize the surface. The following reduction was conducted at 400^0C for 10 hrs under 50 ml/min H_2 flow.

4.3. Kinetic Study of Preferential CO Oxidation over Pt- Sn/AC Catalyst

CO and O_2 conversions and the process parameter for describing oxygen excess, λ, were defined by Eqn 4.1-2-3.

$$X_{CO}(\%) = \frac{[CO]_{in} - [CO]_{out}}{[CO]_{in}} \times 100 \tag{4.1}$$

$$X_{O_2}(\%) = \frac{[O_2]_{in} - [O_2]_{out}}{[O_2]_{in}} \times 100 \tag{4.2}$$

$$\lambda = \frac{2C_{O_2}}{C_{CO}} = \frac{2P_{O_2}}{P_{CO}} \tag{4.3}$$

The amount of liquid water used in the experiments was calculated as below;

$$V_{steam(H_2O)} = \frac{V_{liquid(H_2O)} \times \rho_{H_2O} \times R \times T}{MW_{H_2O} \times P} \quad (4.4)$$

where ρ=1000 $g.L^{-1}$; P=1 atm; R=0.082 $L.atm.mol^{-1}.K^{-1}$; T=298 K and MW_{H2O}=18 $g.mol^{-1}$. The required amount was determined as 0.0074 ml/min. to meet 10% H_2O composition.

CO oxidation experiments, tabulated in Table3.8., were performed to collect intrinsic kinetic data in the initial rates region. The reaction rates, ($-R_{CO}$), were calculated from conversion versus space time (W_{cat}/F_{COin}) data:

$$\left(-R_{CO}\right) = \frac{x_{CO}}{W / F_{CO_{in}}} \quad (4.5)$$

where, x_{CO} symbolizes CO conversion, F_{COin} is inlet CO flow rate in μmol min^{-1}, W_{cat} is the catalyst weight in mg, and ($-R_{CO}$) is the reaction rate in μmol $mg^{-1}min^{-1}$. The space time (mg min μmol^{-1}) was defined as the ratio of mass of catalyst (W_{cat}) to the molar flow rate of CO at the reactor inlet, F_{CO}. Data obtained from CO analyzer at 150 min time-on-stream (TOS) were used in the calculation of reaction rates and kinetic calculations. The reason of using 150 min. TOS data recorded by CO analyzer for CO conversion was to allow time for stabilization in reaction conversion. It should be noted that considering possible fluctuations the average of conversion data recorded between 140 and 150 min. TOS were also used as comparison basis, and the average conversion values confirm 150 min. TOS data. The data obtained from gas chromatograph for 120 min. TOS were used for calculating H_2, CH_4 and O_2 conversion values. The measurement error margin for chromatographic data is below $\pm$ 1%, and that for CO analyzer is below $\pm$ 0.01%.

Fractional CO conversions for experiment 1 and 8 obtained from CO analyzer are shown as examples in Figure 4.1 and Figure 4.2 for λ=2 at W/F_{CO}= 0.0489 and 0.0366 $mg.min.\mu mol^{-1}$ respectively. The discontinuities in the figures results from diverting the

flow to GC for determination of O_2 concentration in the product stream by GC analysis. For each at constant feed composition, CO conversion levels were determined for two space time values in order to confirm the linear characteristic of conversions in the initial rates region. This is demonstrated for several experiments in Appendix A. The CO and O_2 conversion data obtained for each experiment over the 1wt.%Pt-0.25wt.%Sn/AC3 catalyst at 383 K with CO, O_2, CO_2, H_2, H_2O, CH_4 and balance He in the feed are given in Table 4.1. Four different CO and three different O_2 concentration levels were used, and each feed composition was tested at 2 different space times.

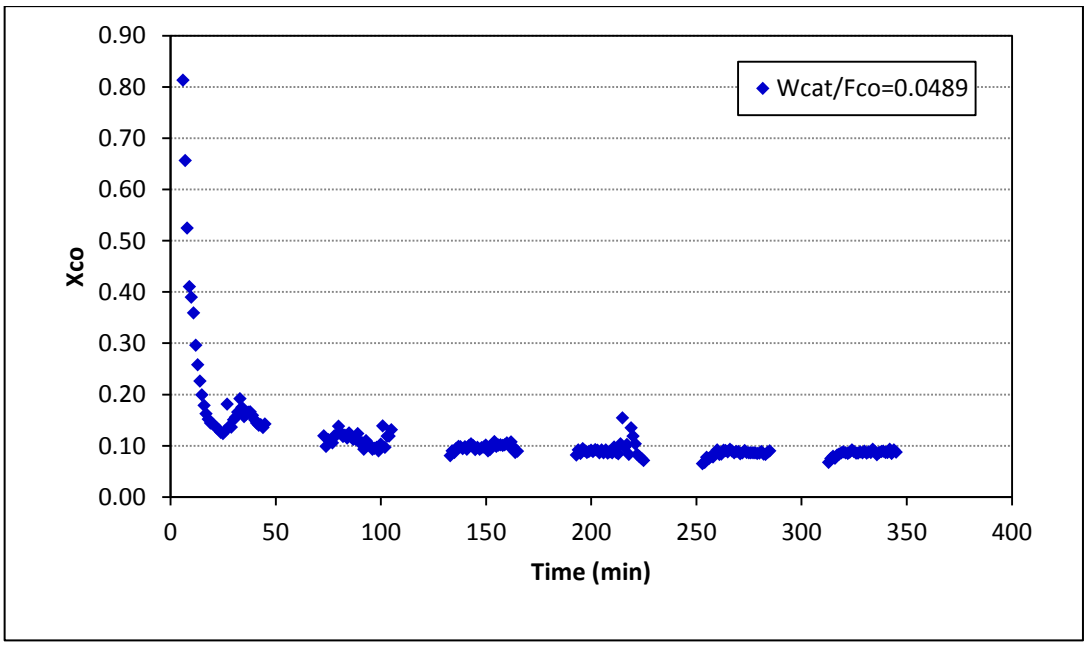

Figure 4.1. Fractional CO conversion vs. time data obtained from CO Analyzer for experiment 1.

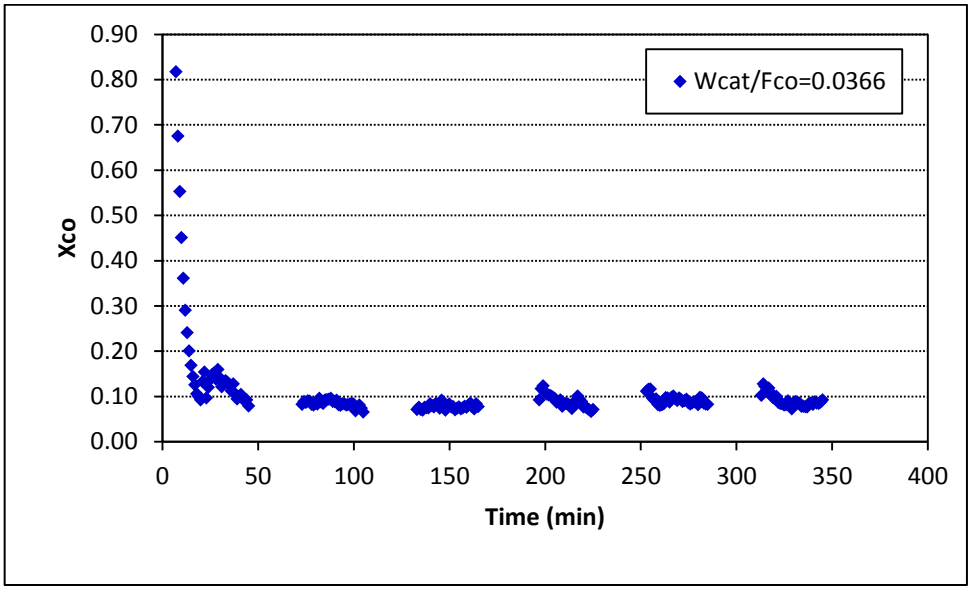

Figure 4.2. Fractional CO conversion vs. time data obtained from CO Analyzer for experiment 8.

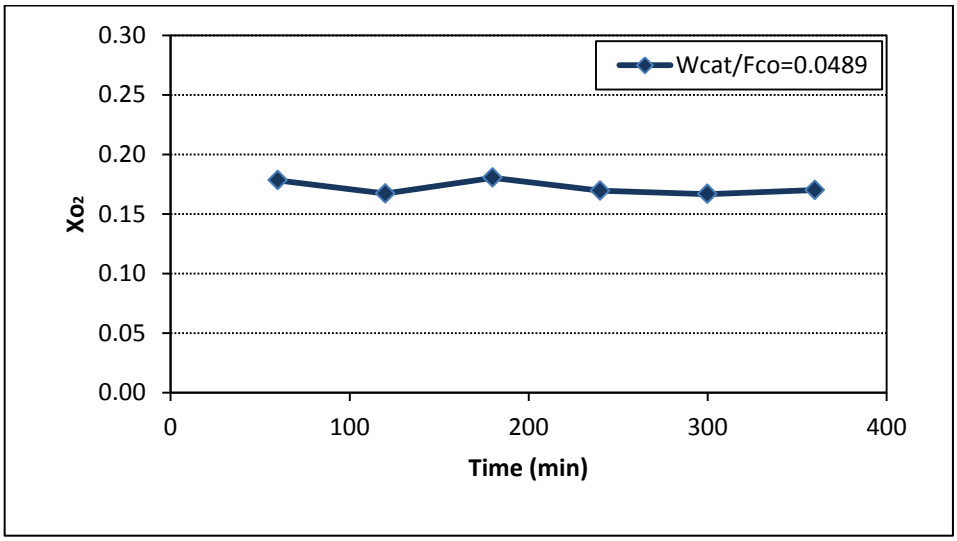

Figure 4.3. Fractional O_2 conversion vs. time data obtained from GC for experiment 1.

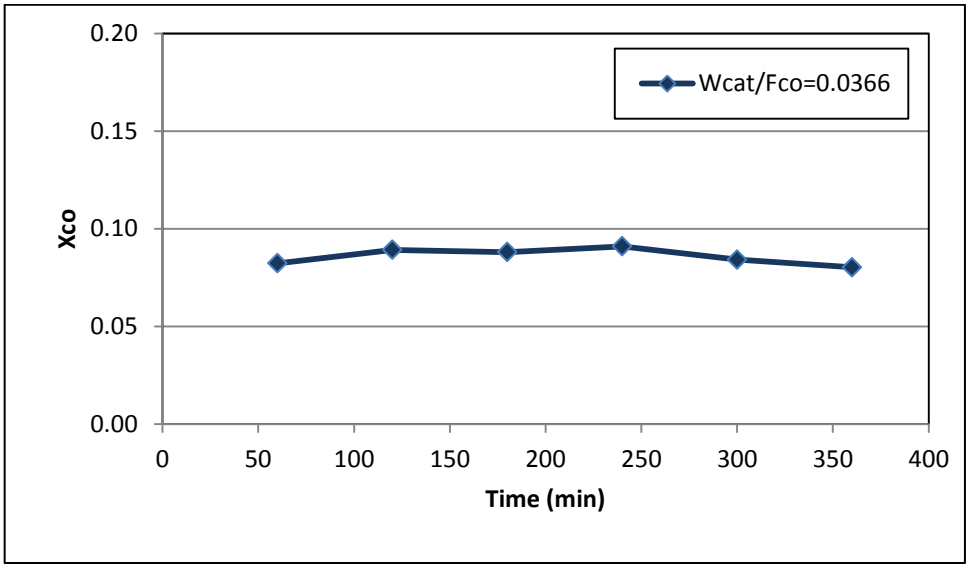

Figure 4.4. Fractional O_2 conversion vs. time data obtained from GC for experiment 8.

Table 4.1. CO and O_2 conversions over 1% Pt- 0.25% Sn/AC3 at T=110^{0}C.

Exp	**W_{cat} (mg)**	**CO (ml/min)**	**O_2 (ml/min)**	**F_{tot} (ml/min)**	**CO conversion**	**O_2 Conversion**
1	20	1	1	100	0.1014	0.167
2	20	1	1.25	100	0.1178	0.153
3	20	1	1.5	100	0.0897	0.059
4	20	1.25	1.25	100	0.0836	0.111
5	20	2	1	100	0.0345	0.136
6	20	2	1.5	100	0.0561	0.076
7	20	2.5	1.25	100	0.0758	0.141
8	15	1	1	100	0.0834	0.089
9	15	1	1.25	100	0.0454	0.079
10	15	1	1.5	100	0.0482	0.044
11	15	1.25	1.25	100	0.0810	0.092
12	15	2	1	100	0.0327	0.083
13	15	2	1.5	100	0.0370	0.049
14	15	2.5	1.25	100	0.0385	0.104

Besides O_2, the concentration of H_2, CO and CH_4 both in the feed and product streams were determined by GC as well; those data were used in calculating conversion and production percentages. On the other hand in calculating CO conversion and flow values, CO analyzer data were used due to the fact that CO concentration values measured by CO Analyzer are more accurate than those measured by GC. The calculated CO, O_2, H_2, and CH_4 conversion values belong to all kinetic experiments are given in Table 4.2. It can be seen from the Table 4.2., H_2, and CH_4 conversions are rather small compared to O_2 and CO conversion values, meaning that CO oxidation is more favorable than H_2 and methane oxidation reactions for the specified conditions used in this study, and those values confirmed that Pt-Sn/AC catalyst is a highly selective catalyst for CO oxidation under realistic feed conditions at 383 K.

Table 4.2. CO, O_2, H_2, and CH_4 conversion values obtained in kinetic experiments.

Exp	**CO conversion**	**O_2 conversion**	**H_2 conversion**	**CH_4 conversion**
1	0.1014	0.167	0.024	0.023
2	0.1178	0.153	~0	0.014
3	0.0897	0.059	~0	~0
4	0.0836	0.111	~0	0.025
5	0.0345	0.136	0.009	0.016
6	0.0561	0.076	~0	0.012
7	0.0758	0.141	0.007	0.022
8	0.0834	0.089	0.004	0.024
9	0.0454	0.079	0.012	0.015
10	0.0482	0.044	0.015	0.017
11	0.0810	0.092	~0	~0
12	0.0327	0.083	~0	0.008
13	0.0370	0.049	0.010	0.015
14	0.0385	0.104	0.001	0.009

4.3.1. Evaluation of Rate Parameters of CO Oxidation

The power-law type rate expression of CO oxidation for realistic feed is given by Eqn 4.6.

$$-r = k\,(P_{CO})^{\alpha}\,(P_{O_2})^{\beta}\,(P_{H_2})^{\psi}\,(P_{H_2O})^{\gamma}\,(P_{CO_2})^{\theta}\,(P_{CH_4})^{\varphi} \tag{4.6}$$

In this study, a simple rate expression, which can be used in sizing the PROX reactor of fuel processor, depends on CO and O_2 is desired. As a consequence, H_2, CO_2, H_2O and CH_4 flow rates were kept constant, i.e. 60% H_2, 15% CO_2, 10% H_2O, and 3% CH_4 respectively in all the set of experiments. Therefore, the power-law type rate expression can be written as below assuming the term $k\left(P_{H_2}\right)^{\psi}\left(P_{H_2O}\right)^{\gamma}\left(P_{CO_2}\right)^{\theta}\left(P_{CH_4}\right)^{\varphi}$ was taken as constant and all related terms are lumped in k' of the rate expression.

$$-r = k'\,(P_{CO})^{\alpha}\,(P_{O_2})^{\beta} \tag{4.7}$$

Evaluation of the rate parameters requires first the determination of reaction rates on the left-hand side of Eqn. 4.7. The reaction rates were calculated from the slopes of the conversion versus residence time graphs. Representative figures were given below for a few experiments. Figure 4.5-8 display conversion levels of each set, which involve two experiments at constant flow and constant feed composition with different catalyst weights, hence different residence times, as indicated in Table 4.1. The rates of experiments determined from the slopes of the CO conversion versus (W_{cat}/F_{CO}) graphs for all kinetic experiments are shown in Table 4.3.

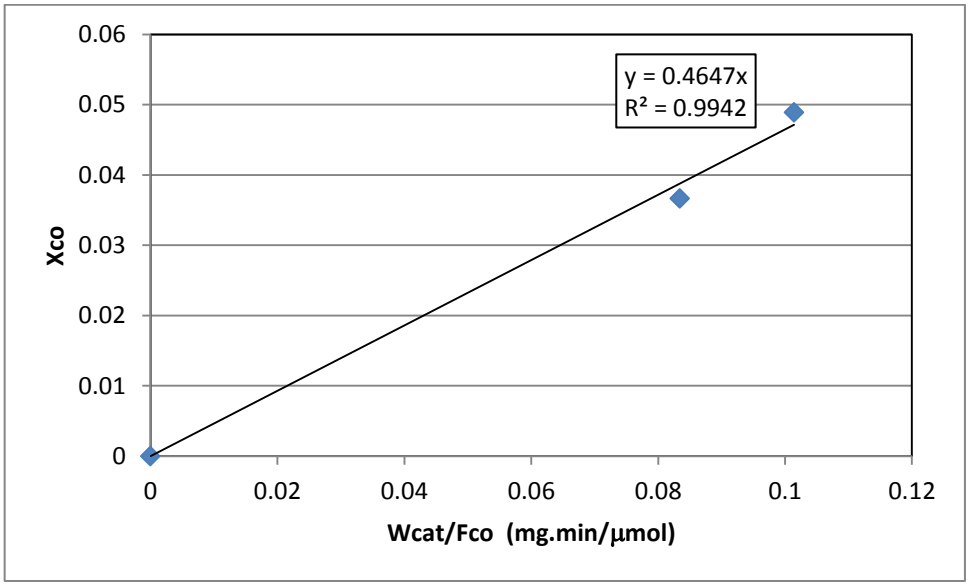

Figure 4.5. Conversion versus residence time plot for experiments 1 and 8 with %1 CO and 1% O_2 composition.

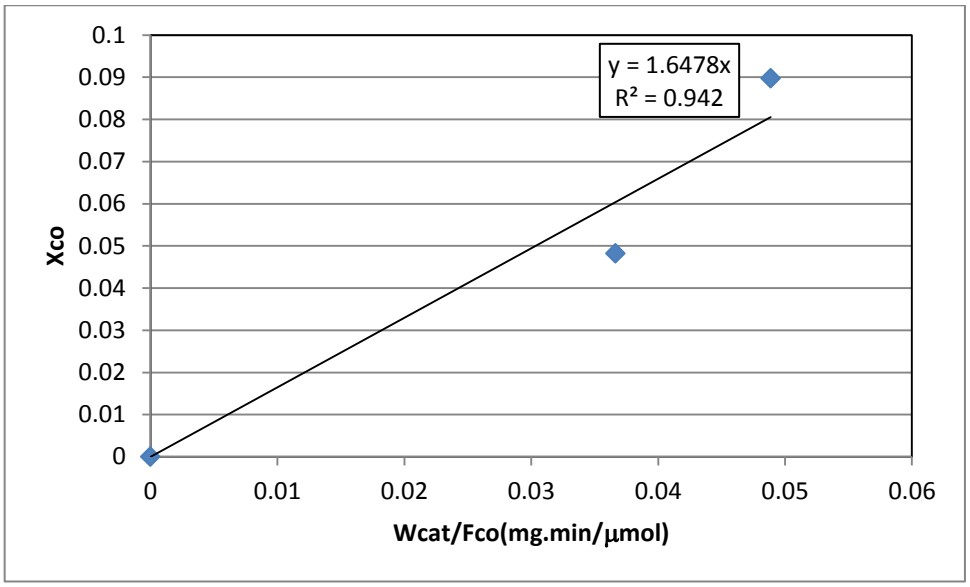

Figure 4.6. Conversion versus residence time plot for experiments 3 and 10 with %1 CO and 1.5% O_2 composition.

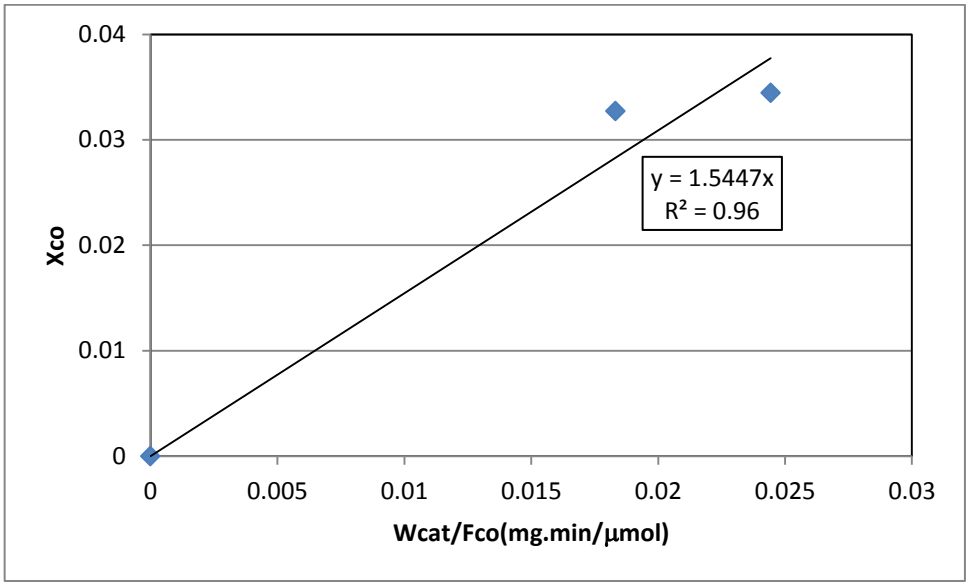

Figure 4.7. Conversion versus residence time plot for experiments 6 and 13 with %2 CO and 1% O_2 composition.

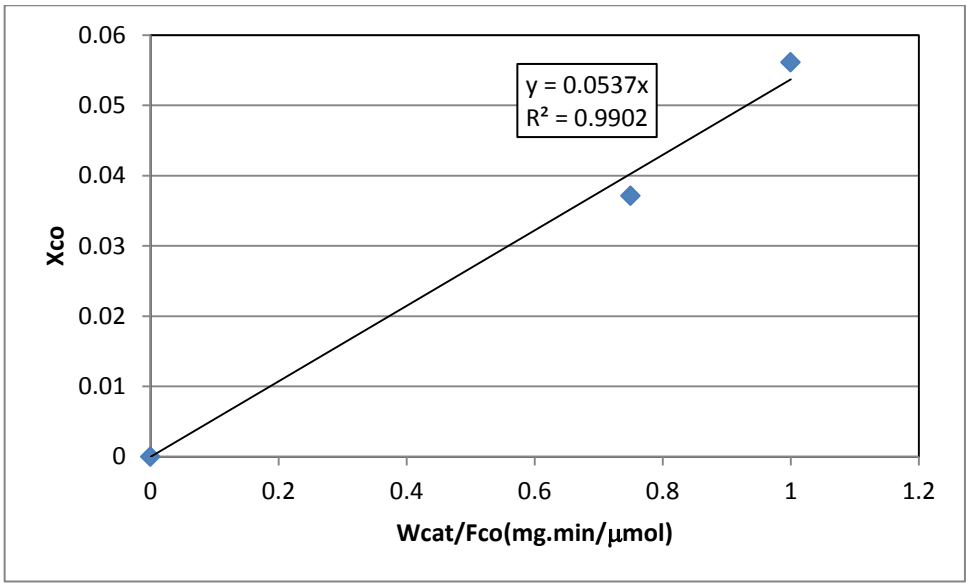

Figure 4.8. Conversion versus residence time plot for experiments 7 and 14 with %2 CO and 1.5% O_2 composition.

Table 4.3. Partial pressure and residence time data for each experiment at 110^0C over 1wt%Pt-0.25wt%Sn/AC3.

Exp	**P_{co} (atm)**	**P_{O2} (atm)**	**W_{cat}/F_{COin} (mg.min.µmol^{-1})**
1	0.01	0.01	0.0489
2	0.01	0.0125	0.0489
3	0.01	0.015	0.0489
4	0.0125	0.0125	0.0391
5	0.02	0.01	0.0244
6	0.02	0.015	0.0244
7	0.025	0.0125	0.0196
8	0.01	0.01	0.0367
9	0.01	0.0125	0.0367
10	0.01	0.015	0.0367
11	0.0125	0.0125	0.0293
12	0.02	0.01	0.0183
13	0.02	0.015	0.0183
14	0.025	0.0125	0.0147

Table 4.4. Initial rate data and goodness of fits for each set of experiment.

Exp	**CO (ml/min)**	**O_2 (ml/min)**	**λ**	**$(-R_{CO})_0$ (µmol mg^{-1} min^{-1})**	**R^2**
1&8	1	1	2	0.2148	0.994
2&9	1	1.25	2.5	0.1988	0.833
3&10	1	1.5	3	0.1648	0.942
4&11	1.25	1.25	2	0.2362	0.953
5&12	2	1	1	0.1545	0.960
6&13	2	1.5	1.5	0.2198	0.990
7&14	2.5	1.25	1	0.3428	0.925

The CO and O_2 partial pressures used in the experiment and the CO consumption rates calculated were processed by using nonlinear regression analysis. "Lsqnonneg" function provided in the computer software MATLAB was used in order to estimate the parameters, k, α and β of Equation 4.6. The sum of the squared differences of the measured reaction rates, and the calculated reaction rates, was found to be 0.1019 μmol mg^{-1} min^{-1}.

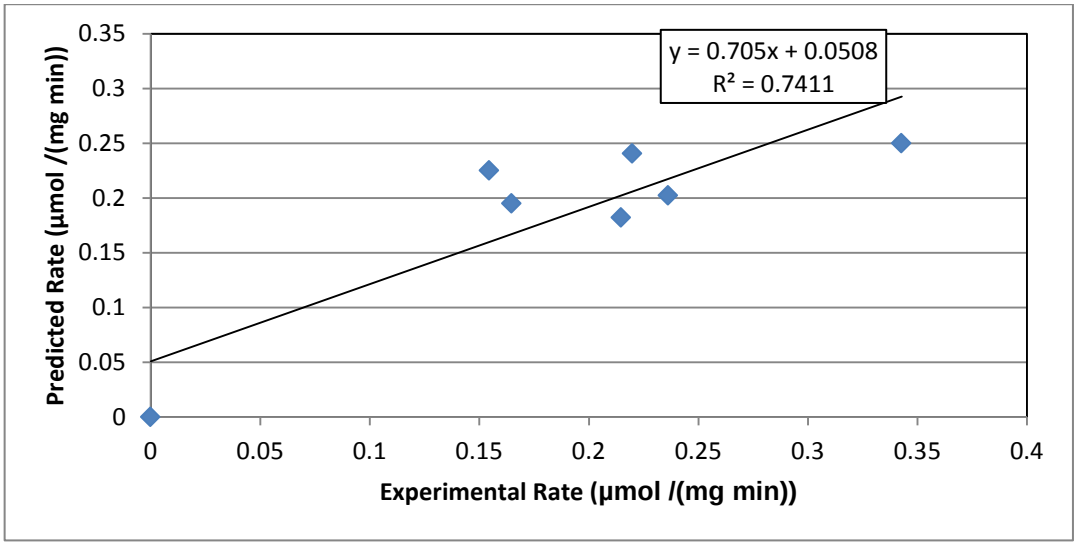

Figure 4.9. Experimental rates versus calculated rates of low-temperature CO oxidation over 1 wt.%Pt-0.25wt.%Sn/AC3.

The suggested kinetic model gives the rate expression with respect to only CO and O_2 partial pressures. The rest of the equation was assumed to be constant. The R^2 values showing goodness of fit (0.741) indicates that the calculated values do not fit the measured rates perfectly. Considering the very high R^2 values confirming linearity for "X_{CO}-W_{cat}/F_{CO}" graphs used in rate calculations, the most plausible reason for relatively low R^2 value in non-linear analysis is the fact that although H_2, CO_2, H_2O, CH_4 flow rates were kept constant in the feed stream, CO/H_2O, and H_2/O_2 ratios did not remain constant; our DRIFTS tests performed on Pt-Sn/AC catalysts by B. Selen Çağlayan indicate that there may be a secondary oxygen source originating from surface OH^- groups formed upon water activation, and the extent of the role of that mechanism may change especially with CO/H_2O and H_2O/O_2 ratios in the feed (Çağlayan, 2011).

The reaction orders with respect to CO (α) and O_2 (β) were determined as 0.29 and 0.17, respectively, with the assumption that the rate of preferential CO oxidation is proportional to the CO and O_2 partial pressures.

Table 4.5. Estimated Reaction Orders.

	k'(μmol $mg^{-1}min^{-1}$ $kPa^{-0.46}$)	**α (with respect to CO)**	**β (with respect to O_2)**
Reaction Orders	0.1835	0.29	0.17

The experiment 1 was repeated at 120 ^{0}C and 135 ^{0}C in order to estimate the activation energy of the reaction. Activation energy was obtained by taking the logarithm of Arrhenius equation (Eqn 4.8); the linearized form of Arrhenius equation (Eqn 4.9), i.e. ln(-r) versus (1/T), was plotted for 110^{0}C and 135^{0}C temperature interval is given in Figure 4.10, resulting from Eqn 4.8. The activation energy calculated from the slope of the straight line in Figure 4.10 ($-E_A/R$) was found as 42.3 kJ mol^{-1}. The frequency factor (k_0) was calculated as $1.44\times10^5\ \mu mol\ mg^{-1}\ \min^{-1}\ kPa^{-0.46}$.

$$k' = k_0\ e^{-\frac{E_A}{RT}} \tag{4.8}$$

$$\ln(-r) = \ln(k_0) - \frac{E_A}{RT} + \alpha \ln(P_{CO}) + \beta \ln(P_{O_2}) \tag{4.9}$$

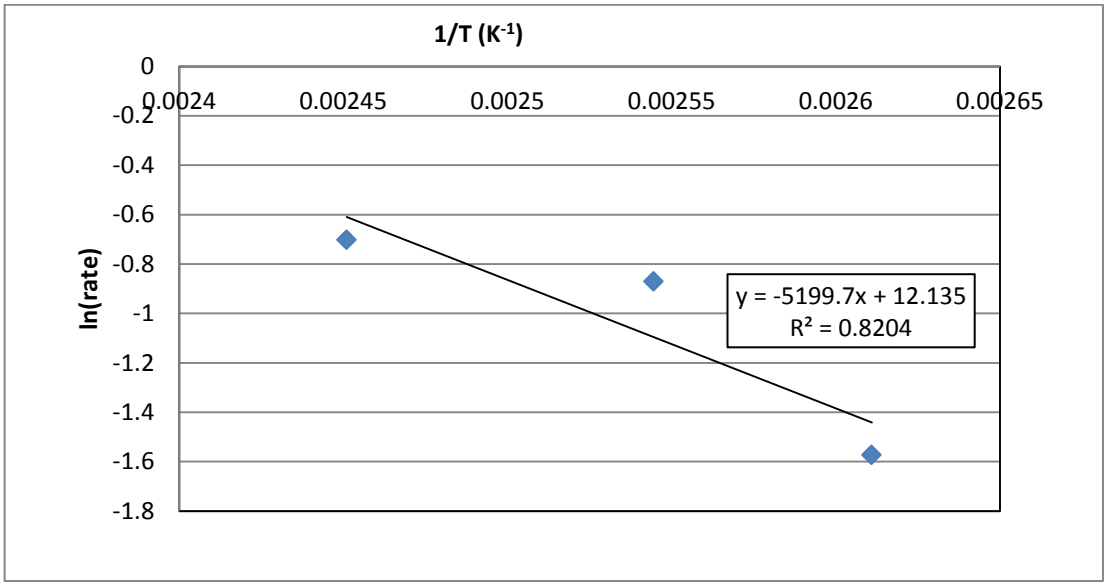

Figure 4.10. Arrhenius plot of PROX.

Consequently, the power-law rate expression for preferential CO oxidation over HNO_3-oxidized activated carbon supported 1wt.%Pt-0.25wt.%Sn/AC catalyst at 383 K in the initial rate region can be given as:

$$-r_{CO} = 1.44\times10^{5}\, e^{-\frac{42.3}{RT}} P_{CO}^{0.29} P_{O_2}^{0.17} \qquad (4.10)$$

This power-law model rate expression is valid, for CO concentration range is 1-2.5% and O_2 composition is 1-1.5%. As CO/H_2O, H_2/O_2, and H_2/H_2O ratios also affect the rate of reaction, obtained equation can be used only when H_2, CO_2, H_2O, CH_4 flow rates are fixed at 60%, 15%, 10%, 3% respectively.

4.3.2. The Effect of CO Flow rate on CO Conversion in the presence of H_2, H_2O, CO_2, and CH_4

The comparative analysis of data presented in Tables 4.6-7 indicate that increase in CO flow rate led to a decrease in CO conversion level, and the extent of conversion level decrease change with oxygen partial pressure level and the values of λ. As an example, for fixed O_2 partial pressure, 0.01 atm, doubling CO flow rate led to a ca. 65% decrease in CO conversion level, i.e. from 0.1014 to 0.0345 (Table 4.6) when λ was decreased from 2 to 1.

On the other hand, for fixed oxygen partial pressure at 0.015 atm, doubling the CO flow rate led to a rather limited decrease, ca. 37%, in CO conversion when λ was decreased from 3 to 1.5.

Table 4.6. CO conversion levels of experiment 1 and 6.

Exp	**CO (ml/min)**	**O_2 (ml/min)**	**CO Conversion**
1	1	1	0.1014
6	2	1	0.0345

Table 4.7. CO conversion levels of experiment 3, 4 and 7.

Exp	**CO (ml/min)**	**O_2 (ml/min)**	**CO Conversion**
3	1	1.5	0.0897
4	1.2	1.5	0.0843
7	2	1.5	0.0561

5. CONCLUSIONS AND RECOMMENDATIONS

5.1. Conclusions

The PROX kinetics over HNO_3-oxidized activated carbon supported 1wt% Pt-0.25wt%Sn/AC catalyst prepared by sequential impregnation was studied under fully realistic conditions with the feed having H_2, CO_2, CH_4 and H_2O. The reactor feed had a range of CO (1-2.5%) and O_2 (1-1.5%) flows corresponding to oxygen excess factors between 1 and 3. The flow rates of H_2, CO_2, CH_4 and H_2O were kept constant in order to obtain the orders of power-law type kinetic expression with respect to CO and O_2.

Intrinsic kinetic data were obtained in the initial rates region at 110^0C using multivariable non-linear optimization function of MATLAB. The results of the optimization showed that a simple power-law rate equation with reaction orders of 0.29 for CO and 0.17 for O_2 can describe preferential CO oxidation over 1wt.%Pt-0.25wt.%Sn/AC3 at 383 K in the presence of H_2, CO_2, H_2O, and CH_4. The positive reaction order of CO and O_2 indicates that the CO and O_2 coverage are below saturation under the reaction conditions and, therefore, a decrease in partial pressure of CO and O_2 will also decrease the reaction probability for CO oxidation. The activation energy of preferential CO oxidation was found to be 42.3 kJ mol^{-1} in a temperature range of 110^0C-135^0C.

As the calculated orders with respect to CO and O_2 in the current study are widely different from the previous one on the same catalyst with a feed having only CO and O_2, which were 0.96 and (-0.31), respectively; the crucial importance of having a kinetic expression, which is valid for real feed, in the PROX reactor design has been confirmed.

As CO/H_2O, H_2/O_2, and H_2/H_2O ratios may also affect the reaction kinetics, the power type rate equation can be safely used only when H_2, CO_2, H_2O, CH_4 concentrations in the feed do not significantly deviate from 60%, 15%, 10%, 3%, respectively.

5.2. Recommendations

Regarding the results of present work, the following points are thought worthwhile for future studies on the kinetics preferential CO oxidation:

Besides the power-law kinetic model, Langmuir Hinshelwood Hougen-Watson type model under realistic conditions may be also investigated for preferential CO oxidation although it will be difficult for the feed including the gases H_2, CO_2, H_2O, CH_4.

The effects of H_2, CO_2, H_2O concentrations can also be investigated by changing one of them while keeping the others constant, in order to predict the effects of H_2/O_2, CO/H_2O, and H_2/H_2O ratios in the feed.

Experiments can be performed with more than two residence times in order to be more accurate.

APPENDIX A: CONVERSION VERSUS RESIDENCE TIME GRAPHS

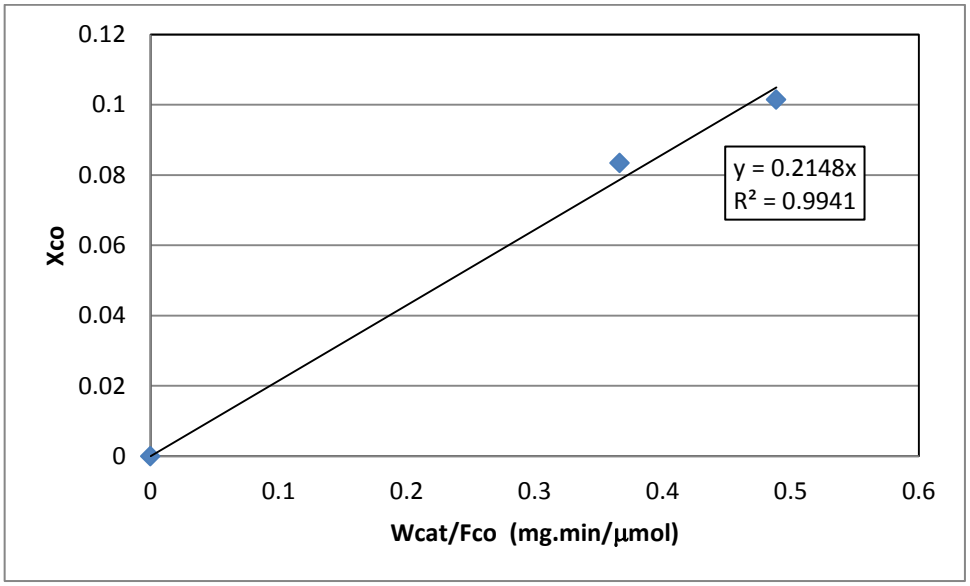

Figure A.1. Fractional CO conversion vs. residence time graph of experiments 1 and 8.

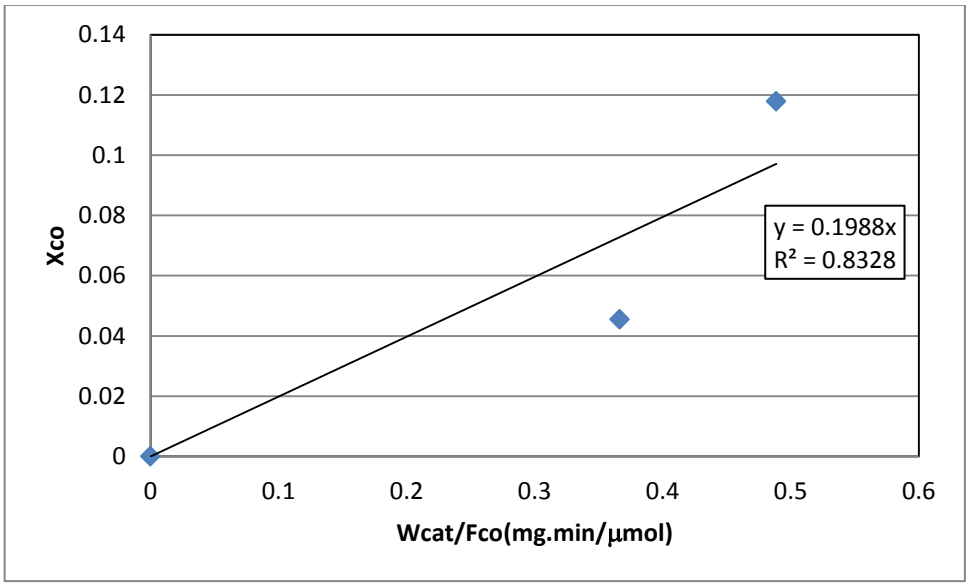

Figure A.2. Fractional CO conversion vs. residence time graph of experiments 2 and 9.

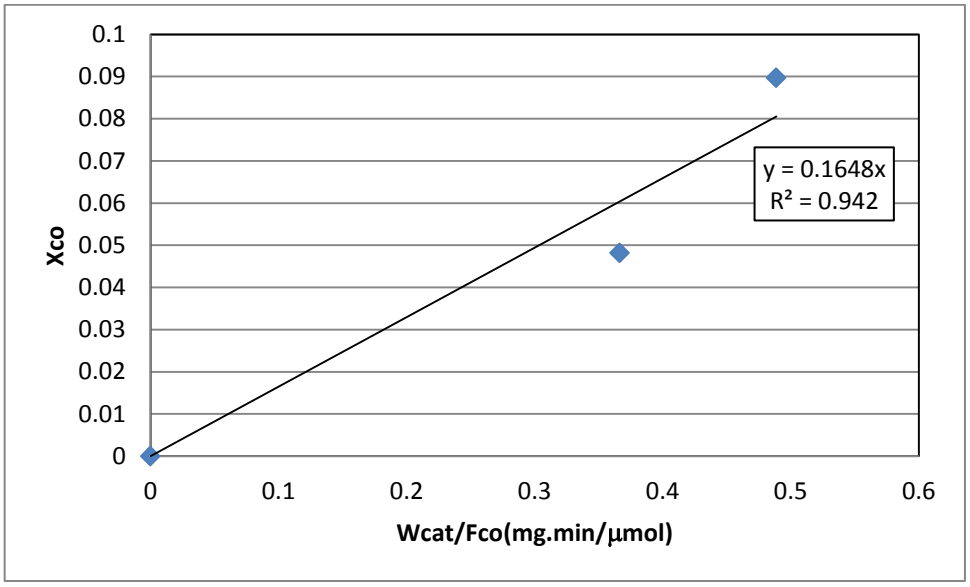

Figure A.3. Fractional CO conversion vs. residence time graph of experiments 3 and 10.

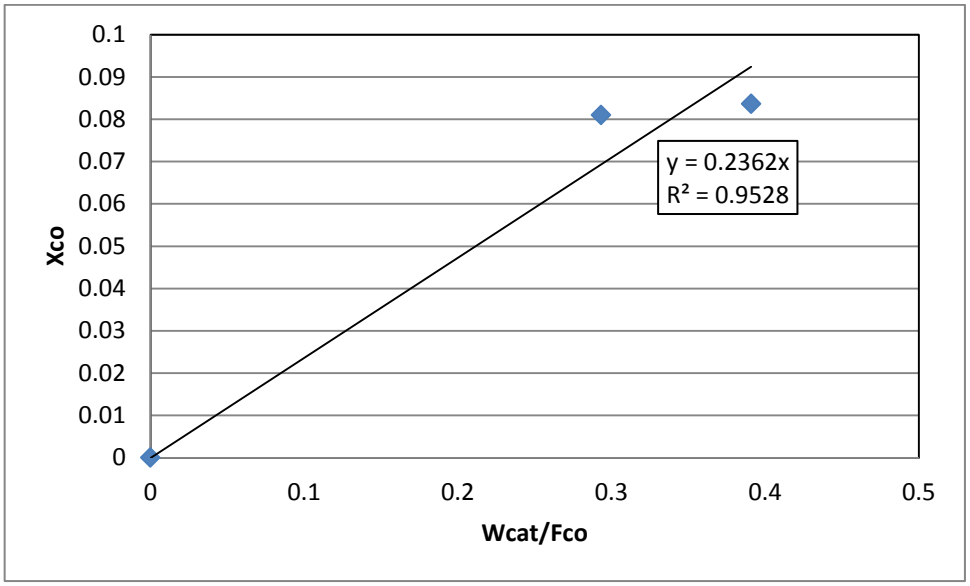

Figure A.4. Fractional CO conversion vs. residence time graph of experiments 4 and 11.

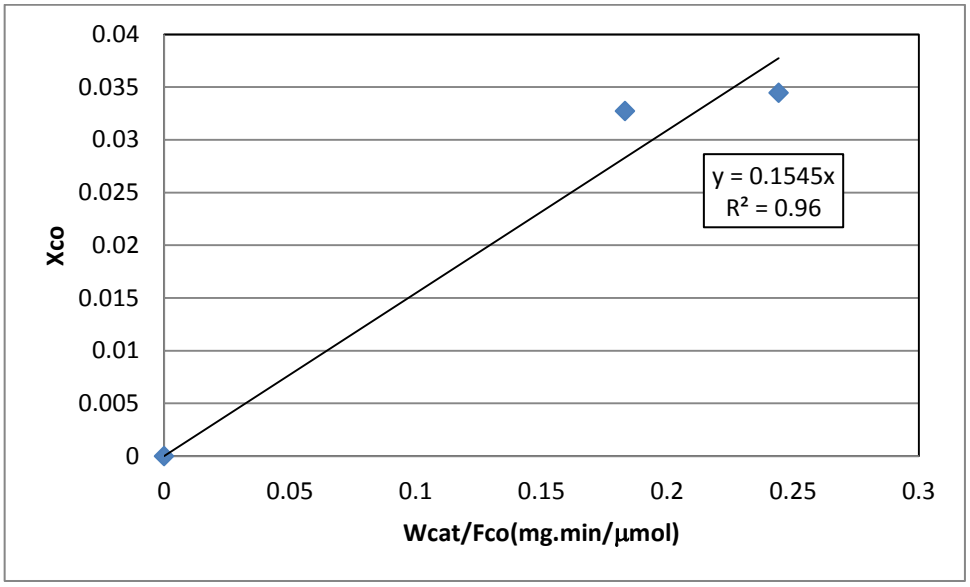

Figure A.5. Fractional CO conversion vs. residence time graph of experiments 5 and 12.

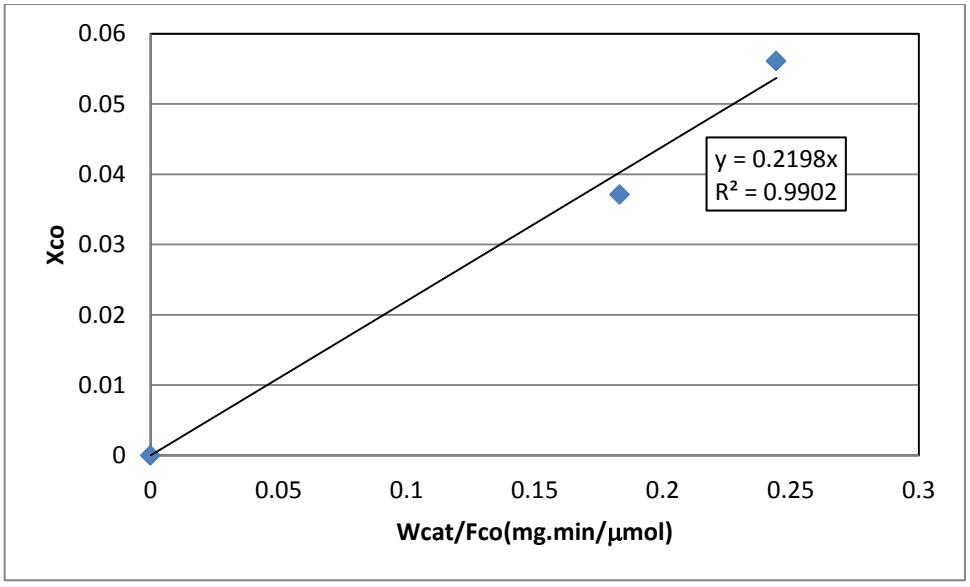

Figure A.6. Fractional CO conversion vs. residence time graph of experiments 6 and 13.

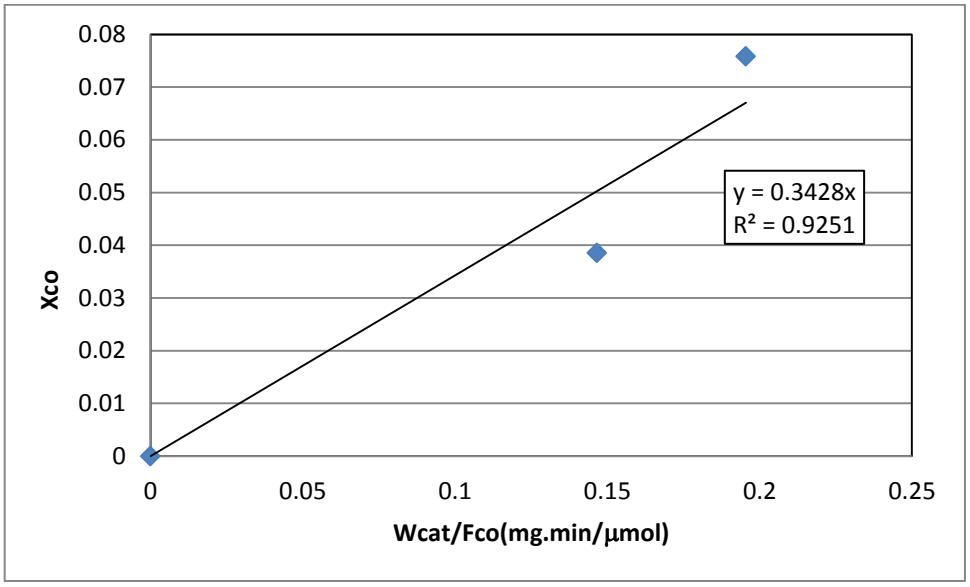

Figure A.7. Fractional CO conversion vs. residence time graph of experiments 7 and 14.

REFERENCES

Akın, A. N., 1996, *Development of Coprecipitated Cobalt-Alumina Catalysts for the Production of C1-C4 Hydrocarbons by Carbon Monoxide Hydrogenation*, Ph.D. Dissertation, Bogaziçi University.

Aksoylu A. E., M. Madalena, A. Freitas, J. L. Figueiredo, 2000, " Bimetallic Pt–Sn catalysts supported on activated carbon I. The effects of support modification and impregnation strategy", *Applied Catalysis A: General*, Vol. 192, pp. 29–42.

Aksoylu A. E., M. Madalena, A. Freitas, J. L. Figueiredo, 2000, " Bimetallic Pt–Sn catalysts supported on activated carbon. II. CO oxidation", *Catalysis Today*, Vol. 62, pp. 337-346.

Aksoylu A. E., M. Madalena, A. Freitas, M. Fernando, R. Pereira, J. L. Figueiredo, 2001, "The effects of different activated carbon supports and support modifications on the properties of Pt/AC catalysts", *Carbon*, Vol. 39, pp. 175–185.

Atalik B., D. Uner, 2006, " Structure sensitivity of selective CO oxidation over Pt/γ - Al_2O_3", *Journal of Catalysis*, Vol. 241, pp. 268–275.

Auer E., A. Freund, J. Pietsch, T. Tacke, 1998, "Carbons as supports for industrial precious metal catalysts", *Applied Catalysis A*, Vol. 173, pp. 259-271.

Avcı, A. K., Z. İ. Önsan and D. L. Trimm, 2001, "On-board Fuel Conversion for Hydrogen Fuel Cells: Comparison of Different Fuels by Computer Simulations", *Applied Catalysis A: General*, Vol. 216, pp. 243-256.

Ayastuy J.L., A. Gil-Rodríguez, M.P. González-Marcos, M.A. Gutiérrez-Ortiz, 2006," Effect of Process Variables on Pt/CeO_2 Catalyst Behaviour for the PROX Reaction", *International Journal of Hydrogen Energy*, Vol. 31, pp. 2231–2242.

Baltacıoglu F.S., B. Gülyüz, A. E. Aksoylu, Z. İ. Önsan, 2007, "Low Temperature CO Oxidation Kinetics over Activated Carbon Supported Pt-SnO_x Catalysts", *Turk J Chem,* Vol. 31, pp. 455–464.

Bissett Edward J., H. Oh Se, R. M. Sinkevitch, 2005, "Pt Surface Kinetics for a PrOx Reactor for Fuel Cell Feedstream Processing", *Chemical Engineering Science,* Vol. 60, pp. 4709–4721.

Caputo, T., R. Pirone and G. Russo, 2006, "Supported CuO/Ce1−xZrxO_2 catalysts for the preferential oxidation of CO in H_2-rich gases", *Kinetic and Catalysis,* Vol. 47, pp. 756-764.

Caputo T., L. Lisi, R. Pirone, G. Russo, 2007, "Kinetics of the Preferential Oxidation of CO over CuO/CeO_2 Catalysts in H_2-Rich Gases", *Ind. Eng. Chem. Res,* Vol. 46, pp. 6793-6800.

Cormos Calin-Cristian, 2011," Hydrogen Production from fossil fuels with carbon capture and storage based on chemical looping systems", *International Journal of Hydrogen Energy,* Vol. 36, pp. 5960-5971.

Çağlayan B. Selen, 2011, *" Design and Development of Catalysts & Adsorbents for CO_x Free H_2 Production ",* Ph.D. Dissertation, Boğaziçi University.

Ersöz A., H. Olgun, S. Ozdoğan, 2006, "Reforming Options for Hydrogen Production from Fossil Fuels for PEM fuel cells", *Journal of Power Sources*, Vol. 154, pp. 67-73.

Gülyüz B., Ş. Ö. Aydınoğlu, A. E. Aksoylu, Z. İ. Önsan, 2009, "Kinetics of CO oxidation over Pt-CeO_x supported on air-oxidized activated carbon", *Turk J Chem,* Vol. 33, pp. 589–598.

Kevin McGrail, *The Online Fuel Cell Information Resource*, http://www.fuelcells.org/, 06.05.2011.

Kipnis M., E. Volnina, 2010, “New approaches to preferential CO oxidation over noble metals”, *Applied Catalysis B*, Vol. 98, pp. 193–203.

Kolb, G., V. Hessel, V. Cominos, C. Hofmann, H. Löwe, *et al.*, 2007, “Selective Oxidations in Micro-Structured Catalytic Reactors-For Gas-Phase Reactions and Specifically for Fuel Processing for Fuel Cells”, *Catalysis Today*, Vol. 120, pp. 2-20.

Koroneos C., A. Dompros, G. Roumbas, N. Moussiopoulos, 2004, "Life cycle assessment of hydrogen fuel production processes", *International Journal of Hydrogen Energy*, Vol. 29, pp. 1443-1450.

Lobera M.P., C. Tellez , J. Herguido, M. Menendez, 2010, “Catalytic purification of H_2-rich streams by CO-PROX over Pt-Co-Ce/γ-Al_2O_3 in fluidized bed reactors”, *Catalysis Today*, doi:10.1016/j.cattod.2010.01.051.

Mariño F., C. Descorme, D. Duprez, 2004, “Noble metal catalysts for the preferential oxidation of carbon monoxide in the presence of hydrogen (PROX)”, *Applied Catalysis B*, Vol. 54 , pp. 59–66.

Moreno M., Graciela T. Baronetti, Miguel A. Laborde, Fernando J. Marino, 2008, “Kinetics of preferential CO oxidation in H_2 excess (COPROX) over CuO/CeO_2 catalysts”, *International Journal of Hydrogen Energy*, Vol. 33, pp. 3538–3542.

Özkara Ş., A. E. Aksoylu, 2003, “Selective low temperature carbon monoxide oxidation in H_2-rich gas streams over activated carbon supported catalysts”, *Applied Catalysis A*, Vol. 251, pp. 75–83.

Park E. D., D. Lee, H. C. Lee, 2009, “Recent progress in selective CO removal in a H_2-rich stream”, *Catalysis Today*, Vol. 139, pp. 280–290.

Polster C. S, R. Zhang, M. T. Cyb, J. T. Miller, C. D. Baertsch, 2010, "Selectivity loss of Pt/CeO_2 PROX catalysts at low CO concentrations: mechanism and active site study", *Journal of Catalysis*, Vol. 273, pp. 50–58.

Ratnasamy P., D. Srinivas, C.V.V. Satyanarayana, P. Manikandan, R.S. Senthil Kumaran, M. Sachin, and Vasudev N. Shetti, 2004, " Influence of the support on the preferential oxidation of CO in hydrogen-rich steam reformates over the $CuO–CeO_2–ZrO_2$ system", *Journal of Catalysis*, Vol. 221 pp. 455–465.

Schubert M. M., M. J. Kahlich, G. Feldmeyer, M. Huttner, S. Hackenberg, H. A. Gasteiger., R.J. Behm, 2001, "Bimetallic PtSn catalyst for selective CO oxidation in H_2-rich gases at low temperatures", *Phys. Chem. Chem. Phys.*, Vol. 3, pp. 1123-1131.

Schubert M. M., A. Venugopal, M. J. Kahlich, V. Plzak, R. J. Behm, 2004, "Influence of H_2O and CO_2 on the selective CO oxidation in H_2-rich gases over $Au/\alpha\text{-}Fe_2O_3$", *Journal of Catalysis*, Vol. 222, pp. 32–40.

Schumacher B., Y. Denkwitz, V. Plzak, M. Kinne, R.J. Behm, 2004, "Kinetics, mechanism, and the influence of H_2 on the CO oxidation reaction on a Au/TiO_2 catalyst", *Journal of Catalysis*, Vol. 224 , pp. 449–462.

Siri G.J., G.R. Bertolini, O.A. Ferretti, 2007, "Preferential Oxidation of CO in Presence of H_2 Behavior of $PtSn/\gamma\text{-}Al_2O_3$ Catalysts Modified by K or Ba", *Latin American Applied Research*, Vol. 37, pp. 275-281.

Suh D.J. , Chan Kwak, Jin-Hong Kim, Se Mann Kwon, Tae-Jin Park, 2005, "Removal of carbon monoxide from hydrogen-rich fuels by selective low-temperature oxidation over base metal added platinum catalysts", *Journal of Power Sources*, Vol. 142 pp. 70–74.

Sopeña D., A. Melgar, Y. Briceño, Y. M. Navarro, M.C. Âlvârez-Galvan, F. Rosa, 2007, "Diesel Fuel Processor for Hydrogen Production for 5 kW Fuel Cell Application", *International Journal of Hydrogen Energy*, Vol. 32, pp. 1429-1436.

Soykal Ilgaz, 2006, *"Preferential Oxidation Performance of Pt-Sn/AC Catalysts"*, M.S. Thesis, Boğaziçi University.

Şimşek E., Ş. Özkara, A. E. Aksoylu, Z. İ. Önsan, 2007, "Preferential CO oxidation over activated carbon supported catalysts in H_2-rich gas streams containing CO_2 and H_2O", *Applied Catalysis A,* Vol. 316 pp. 169–174.

Trimm D.L., 2005, "Minimisation of carbon monoxide in a hydrogen stream for fuel cell application", *Applied Catalysis A*, Vol. 296, pp. 1–11.

Trimm, D. L. and Z. İ. Önsan, 2001, "Onboard Fuel Conversion for Hydrogen-Fuel-Cell-Driven Vehicles", Catalysis Reviews-Science and Engineering, Vol. 43 (1-2), pp. 31-84.

Uysal G., A. N. Akın, Z. İ. Önsan, R. Yıldırım, 2006, "Preferential CO oxidation over Pt–SnO_2/Al_2O_3 in hydrogen rich streams containing CO_2 and H_2O (CO removal from H_2 with PROX)", *Catalysis Letters*, Vol. 111, pp. 173-176.

Wang L., Y. Zhou, Q. Liu, Y. Guo, G. Lu, 2010, " Effect of surface properties of activated carbon on CO oxidation over supported Wacker-type catalysts", *Catalysis Today*, Vol. 153, pp. 184–188.